

POLITECNICO DI TORINO

Master's Degree in Mechanical Engineering



**Politecnico
di Torino**



Master's Degree Thesis

Implementation of a new production process for an industrial FDM printer and its characterization at Punch Torino S.p.A.

Prof. Cristiana DELPRETE

Andrea CAFFARATTI

Prof. Chiara GASTALDI

Ing. Bruno CASSAR SCALIA

Ing. Valerio AMETRANO

Academic Year 2021/2022

Summary

The aim of this thesis is the implementation of a production process for a FDM 3D printer at *Punch Torino S.p.A.*, the analysis of its performance and the characterization of the tensile properties of two materials, ULTEM™ and Carbon PEEK. In the first part of the document, a brief introduction on Additive Manufacturing techniques is present, with a focus on Fused Deposition Modelling, followed by a description of the host company and of the materials that have been studied. Then, the results of the capability assessment of the printer are reported: the study was done following the norm ISO/ASTM 52902:2019. Finally, several specimens were tested following ASTM D638-2014 to determine the tensile properties of the materials and define how they change by varying three parameters: printing orientation (horizontal or vertical), infill rate (100% or 35%) and testing temperature (ambient or 120°C). All the artifacts were created using a *Roboze Argo 500* printer at *Punch Torino*, and the tensile tests were conducted at Politecnico di Torino (DIMEAS).

Acknowledgements

Alle professoresse Cristiana Delprete e Chiara Gastaldi, per l'aiuto che mi hanno dato in questi mesi,

Ai miei tutor aziendali, Bruno Cassar Scalia e Valerio Ametrano, perchè senza di loro questo lavoro sarebbe stato impossibile, e alla *Punch* per avermi dato la possibilità di svolgere il progetto,

Ai miei genitori e a mio fratello, ai miei nonni ed ai miei amici, per avermi accompagnato in questo percorso, ciascuno a modo suo,

Grazie!

Table of Contents

List of Tables	VIII
List of Figures	X
1 Introduction	1
1.1 Introduction to Additive Manufacturing	1
1.2 AM techniques	2
1.3 Fused Deposition Modelling	4
1.3.1 Description of the process	4
1.3.2 Materials	6
1.3.3 Advantages and Limits of FDM	8
1.3.4 Industrial Applications and Prospects	9
2 Equipment and Materials	13
2.1 Additive LAB at <i>Punch Torino S.p.A.</i>	13
2.2 <i>Roboze Argo 500</i>	14
2.3 Materials	15
2.3.1 Carbon PEEK	15
2.3.2 ULTEM™9085	17
3 Capability Assessment	19
3.1 Introduction	19
3.2 <i>Roboze Argo 500</i>	20
3.2.1 Post-installation Capability Assessment: Ultra-PLA	20
3.2.2 Results and Analysis	24
3.3 Capability Assessment for comparison between different materials	28
3.3.1 Capability Assessment: ULTEM™and Carbon-PEEK	34
3.3.2 Results and Analysis	46
4 Tensile Tests	49
4.1 Introduction	49

4.1.1	Parameters	49
4.2	ASTM D638	52
4.3	Printing and Testing	56
4.4	Results and Comments	61
4.4.1	Load vs Displacement diagrams	61
4.4.2	Stress vs Strain diagrams - Carbon PEEK	62
4.4.3	Stress vs Strain diagrams - ULTEM™	66
4.4.4	Results and Analysis	69
5	Conclusions	77
A	Capability Assessment	79
B	Measures of the specimens	83
	Bibliography	85

List of Tables

2.1	Extract of the Carbon PEEK Technical Data Sheet	16
2.2	Adopted parameters for Carbon PEEK	17
2.3	Extract of the ULTEM™ Technical Data Sheet	17
2.4	Adopted parameters for ULTEM™	18
3.1	PLA: thickness resolution ribs artifact	26
3.2	PLA: resolution slotted angles artifact - X axis	26
3.3	PLA: resolution slotted angles artifact - Y axis	27
3.4	PLA: circular artifact	27
3.5	PLA: X-axis resolution artifact	27
3.6	PLA: Y-axis resolution artifact	28
3.7	PLA: vertical resolution artifact	28
3.8	Recap of capability assessments	29
3.9	Measured features and tools	34
3.10	ULTEM™: linear artifact	35
3.11	ULTEM™: circular artifact - medium size	36
3.12	ULTEM™: circular artifact - fine size	36
3.13	ULTEM™: resolution pins artifact - coarse size	36
3.14	ULTEM™: resolution pins artifact - medium size	37
3.15	ULTEM™: resolution holes artifact - coarse size	37
3.16	ULTEM™: resolution holes artifact - medium size	37
3.17	ULTEM™: resolution ribs artifact - coarse size	38
3.18	ULTEM™: resolution ribs artifact - medium size	38
3.19	ULTEM™: resolution slots artifact - coarse size	39
3.20	ULTEM™: resolution slots artifact - medium size	39
3.21	ULTEM™: resolution slotted angles artifact - coarse size	39
3.22	ULTEM™: resolution slotted angles artifact - medium size	40
3.23	ULTEM™: surface texture artifact - medium size	40
3.24	Carbon PEEK: linear artifact	41
3.25	Carbon PEEK: circular artifact - medium size	42
3.26	Carbon PEEK: circular artifact - fine size	42

3.27	Carbon PEEK: resolution pins artifact - coarse size	42
3.28	Carbon PEEK: resolution holes artifact - coarse size	43
3.29	Carbon PEEK: resolution ribs artifact - coarse size	43
3.30	Carbon PEEK: resolution ribs artifact - medium size	43
3.31	Carbon PEEK: resolution slots artifact - coarse size	44
3.32	Carbon PEEK: resolution slots artifact - medium size	44
3.33	Carbon PEEK: resolution slotted angles artifact - coarse size	45
3.34	Carbon PEEK: resolution slotted angles artifact - medium size . . .	45
3.35	Carbon PEEK: surface texture artifact - medium size	45
3.36	Comparison between ULTEM™ and Carbon PEEK - capability assessments	46
4.1	Test matrix	51
4.2	Ultimate dimensions of the specimens	54
4.3	Labels of the specimens	58
4.4	Results of the tensile tests	69
5.1	Capability assessments comparison: Carbon PEEK and ULTEM™ .	77
A.1	Linear artifact	79
A.2	Circular artifacts	80
A.3	Resolution Pins artifact	80
A.4	Resolution Holes artifact	80
A.5	Resolution Ribs artifacts	81
A.6	Resolution Slots artifacts	81
A.7	Resolution Slotted Angles artifacts	82
A.8	Surface Texture artifact	82
B.1	Measures of the specimens for the tensile tests	83

List of Figures

1.1	Scheme of the FDM process	5
1.2	Parameters that influence a FDM process	6
2.1	From left to right: <i>UM S5</i> , <i>MF X7</i> , <i>MF OnyxPro</i>	13
2.2	<i>Roboze Argo 500</i>	14
2.3	Gasket made of Carbon PEEK	16
2.4	Duct made of ULTEM™9085	18
3.1	Thickness resolution ribs artifact (<i>Roboze</i>)	21
3.2	Thickness resolution slot angles artifact (<i>Roboze</i>)	21
3.3	Circular artifact (<i>Roboze</i>)	22
3.4	Resolution X/Y axis artifact (<i>Roboze</i>)	23
3.5	Vertical resolution Z axis artifact (<i>Roboze</i>)	23
3.6	PLA: buildsheet preparation on <i>Simplify 3D</i>	24
3.7	PLA: printed pieces	25
3.8	Linear artifact	30
3.9	Circular artifacts	30
3.10	Resolution pins artifact (medium size)	31
3.11	Resolution holes artifact (medium size)	31
3.12	Resolution ribs artifact (medium size)	32
3.13	Resolution slots artifact (medium size)	32
3.14	Resolution slotted angles artifact (coarse size)	33
3.15	Surface texture artifact	33
3.16	ULTEM™: preparation of the job on <i>Simplify 3D</i>	35
3.17	Carbon PEEK: specimens of the capability assessment	41
4.1	a) Axes directions with respect to the building platform, b) Different building orientations of the same part.	50
4.2	Different infill rates for the same part	51
4.3	Design of the specimen for the tensile test	52
4.4	Reference dimensions for the specimen	52

4.5	Design of the ultimate specimen	53
4.6	Dimensions of the ultimate specimen	54
4.7	Ultra PLA: horizontal (left) and vertical (right) overheated specimen	55
4.8	C-PEEK: vertical specimen with two support towers	55
4.9	Carbon PEEK: broken buildsheet and ruined specimens after the artifacts' removal	56
4.10	ULTEM: complete vertical batch	57
4.11	C-PEEK: four horizontal batches in the printer	57
4.12	a) specimen with extensometer; b) <i>Instron 8801</i> set for high temper- ature tests	59
4.13	Broken specimen at the end of the test	60
4.14	Selection of broken specimens	60
4.15	Batches 1 and 9 - load vs displacement	61
4.16	Carbon PEEK: stress vs strain diagrams	65
4.17	ULTEM TM : stress vs strain diagrams	68
4.18	Values of σ_{break}	70
4.19	Values of E	71
4.20	Values of σ_{yield}	74

Chapter 1

Introduction

1.1 Introduction to Additive Manufacturing

Additive Manufacturing (AM) is a term used to identify a group of productive technologies that build parts by “adding” material layer by layer, differently from traditional processes (milling, drilling. . .) which start from a full piece and create all the features by removing material[1]. The procedure can be generically described as a succession of three steps[2]:

1. Data preparation: a 3D CAD model of the object is designed. Then, by means of specific software, it is converted into a .STL file, i.e., the external surfaces of the part get approximated with a lot of triangles: their number depends on the desired resolution. After this operation, the component gets horizontally sliced and the various layers are created. Eventually, the building instructions are collected into a G-Code which will be used by the machine to print the part(s).
2. Layer-by-layer building: it represents the “real” printing process; the machine follows the commands contained in the G-Code and creates the object. The effective procedure depends on the adopted technology, but in general all of them are based on a building platform that moves down after the creation of each layer to allow the printing of the next one.
3. Post-processing: 3D printed parts must be post-processed so that they respect dimensional tolerances and aesthetical requests. Also, some features, such as holes or threads which require high precision, may be added at the end of the job using different instruments.

Patented in the 1970s, but effectively born in the 1980s, Additive Manufacturing was initially used for creating prototypes and casting mould and tools. Since the

beginning of 21st century, the usage of AM techniques is growing very quickly thanks to continuously evolving resources, which allow to create new processes and improve the already existing ones. Since the parts are built layer by layer, potentially there are no limits regarding the shapes that can be created and this massive design flexibility is one of the main advantages of using these technologies; it allows the building of completely customized parts, and this fact is widely exploited in the biomedical field: for example, a dental implant or a prosthesis can be tailored to each patient[3]. In addition, new opportunities are brought by the constantly increasing number of materials that can be utilized: today, a variety of polymeric [4], metallic and composite materials[5] are available, and cover a wide range of applications. To underline the importance that these technologies will have in the near future, Additive Manufacturing has been included among the drivers of Industry 4.0[6] [7]: this expression was coined in Germany during the 2011 Hannover Fair and it refers to the fourth Industrial Revolution; its main achievement will be the creation of “Smart Factories”: in other words, high-developed plants where all the machines are constantly communicating and collab with each other thanks to wireless connections, cloud-based platforms are employed to store and analyse data, human workers are joined by autonomous robots and other independent devices, and modern technologies, such as AM itself, are widely used.[8]

1.2 AM techniques

During the years, different processes have been developed. They all have both advantages and limitations if compared to the others and it must be highlighted that not all the technologies are suitable for all applications: in fact, depending on the material or on the particular conditions that the product must satisfy, a certain technique should be selected rather than another. The ASTM F42 Committee has collected them into seven categories[9], which will be briefly described in the following:

- Powder Bed Fusion
- Directed Energy Deposition
- Material Extrusion
- Vat Photopolymerization
- Binder Jetting
- Material Jetting
- Sheet Lamination

Powder Bed Fusion Powder Bed Fusion (PBF) techniques exploit a heat source which makes powder particles melt and adhere to each other to form the desired cross section. The source is generally an electron beam or a laser that is directed towards a powder bed which progressively moves down thanks to an elevator, to permit the fusion of a new layer of material after it gets deposited on it. Both metals and polymers can be used.

The products are characterized by fine resolution and high quality; moreover, supports are not needed during printing. However, these techniques are quite slow and costly.[10][11]

Direct Energy Deposition DED techniques are used to print metal parts by contemporarily spraying powder particles in the desired location and melting them; the heat source is either a laser or an electron beam: if the latter is used, the process occurs in a protected environment, thanks to the introduction of inert gases.

These technologies are often used to repair broken objects, by adding material only where it is needed. Completely new items can be built exploiting DED, but they must be post-processed due to poor surface finish. More recent processes substitute the powder with a metallic wire: in this way, wasted material is reduced and efficiency increase (powder particles, when sprayed, do not completely melt).[12][13]

Material Extrusion Material Extrusion techniques print objects by heating a polymeric (sometimes metallic or ceramic) filament to make it softer so it can be extruded using a calibrated nozzle. It is the most common Additive Manufacturing process thanks to its versatility and relatively low cost.[10][11] More details about this technology will be given in Chapter 1.3 of this Thesis, where Fused Deposition Modelling (FDM) will be analysed.

Vat Photopolymerization VP processes create parts by making liquid polymers solidify: some plastics are in fact photosensitive, which means that they cure if they are irradiated by a light source (e.g., UV radiations). This process requires a vat filled with the selected photopolymer (generically called “precursor”) mixed with a photoinitiator, a substance that helps to start the polymerization process when the light irradiates the liquid. The beam’s stimulus causes the solidification of the desired layer; after it, the bottom of the vat moves down and the procedure restarts.[14]

Binder Jetting In this technique, a liquid binder is deposited by a nozzle on a thin layer of powder to impregnate and attach the particles. In this way, the needed cross section is created. The process is similar to the PBF, but it does not rely on heating up the powder; in BJ the particles get glued together, in practice.

Many different materials can be printed this way, such as polymers, metals, ceramics and even sand. However, the resulting part may be very porous, so it needs either an infiltration process or a thermal treatment; furthermore, its mechanical properties are generally poor, so it is usually used only for conceptual prototypes.[11][15]

Material Jetting Material Jetting involves the properties of photopolymers, as VP: the liquid material is deposited on the build platform and immediately cured by means of a light source. Then, the plate goes down and another layer can be created. Since the deposited material is not initially solid, a support material may be necessary, especially to hold up overhang structures. This technique produces low wastes since the deposition of the liquid's droplets is very accurate and the surface quality is high, so it is used especially for conceptual prototypes. This application is enhanced by the fact that MJ machines are able to print coloured materials, so the resulting part can be very realistic and detailed.[16][17]

Sheet Lamination As it can be deduced by its name, Sheet Lamination is an AM technique which consists in bonding together several sheets or foils and then cutting them precisely by using a laser or a mechanical cutter (bond-then-form). The process can also happen in the opposite way (form-then-bond). Sheets are almost always metallic, but also paper can be used. The union of the foils does not involve melting: in fact, they are stuck to each other thanks to the application of some kind of energy (usually coming from an ultrasonic wave) together with mechanical pressure; in case of paper sheets, they are simply glued together. The part often undergoes surface finishing to respect the requested tolerance values.[10][11][15]

1.3 Fused Deposition Modelling

1.3.1 Description of the process

Fused Deposition Modelling (FDM) is an Additive Manufacturing technique based on Material Extrusion. It was patented in 1989 by Scott Crump and the industrial process was firstly introduced two years later by Stratasys, an American company. The process consists in heating and extruding a filament made of thermoplastic material on a building plate. The part is created layer-by-layer, the polymer flows out of a calibrated nozzle (which moves in X and Y directions, following the instructions contained in the G-Code), while the platform moves along Z axis. Some machines are equipped with more than one nozzle, meaning that different filaments can be contemporarily extruded; this property can be conveniently exploited by printing the building material (the one for the part) with one nozzle, and a

compatible support material with the other, facilitating the support removal during the post-processing.[2]

The method is becoming more and more widespread due to the advantages of the thermoplastic materials used, such as cheapness, long life, high toughness, easy to find, recyclability, low shaping temperature, and reshaping when heated. Today, home users can also produce various parts with this method. Due to the simple working principle and low equipment required, the costs of devices producing with the FDM method are lower than the devices used in other AM methods.[5] A scheme of the process is illustrated in fig.1.1 (taken from [18]).

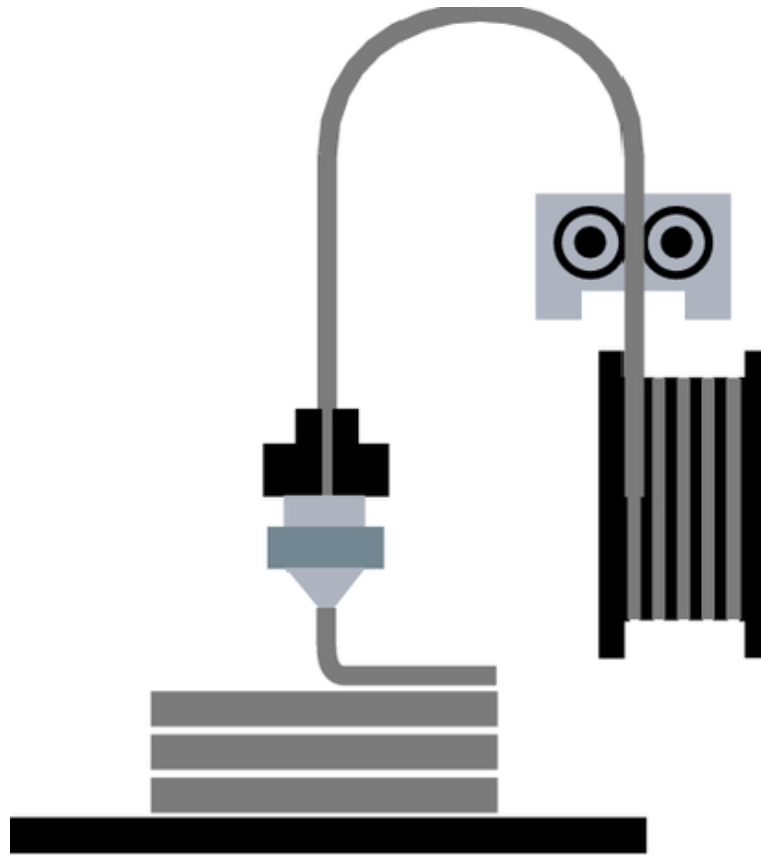


Figure 1.1: Scheme of the FDM process

Many parameters must be taken into account when working with FDM; the combination of them all influence the final result of the job. It is important to set them as well as possible and find the optimal set of values to use, considering pros and cons of each modification: for example, reducing the height of each layer, the surface quality will increase, while the printing time will increase. So, the definition of the parameters shall be adapted based on the piece being printed. Moreover,

mechanical properties are influenced by these variables and the changing of one of them may affect more or less the resistance of the part.[19][20] Fig.1.2 (taken from [20]) shows the several parameters affecting an FDM machine's performance.

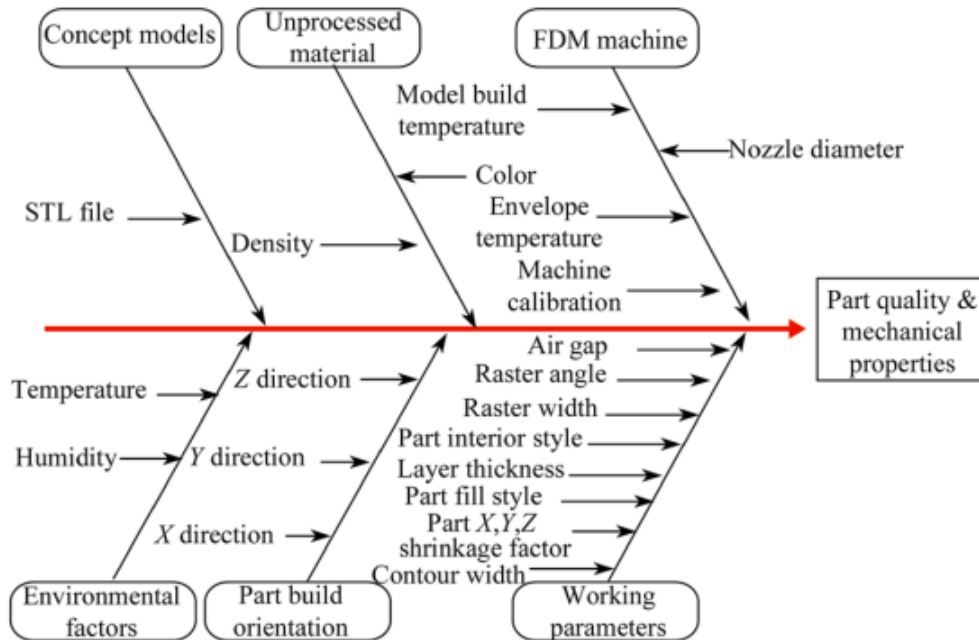


Figure 1.2: Parameters that influence a FDM process

1.3.2 Materials

Many different materials can be printed by FDM machines: polymers are the most used, but also metals, ceramics and composites are available. Two essential conditions must be satisfied by a material to make it suitable for FDM: 1) it should be possible to store it in filament form, wrapped around a coil, and 2) when heated, it should melt in order to extrude it using a nozzle.

Polymers They represent the first materials that have been used for FDM printing and nowadays are the most frequently used. By definition, a polymer is a large molecule made up of chains or rings of linked repeating units (monomers); two categories can be individuated: natural polymers (e.g., silk, rubber, etc.) and synthetic ones[21]. The latter can be further divided into thermosets and thermoplastics. Thermoplastic (or thermosoftening) polymers are suitable for FDM technique since they can be easily softened and re-shaped by heating them; in fact, there are no chemical bonds between different thermoplastic

chains, but only intermolecular forces. Thanks to this characteristic, they can be stored as filaments, heated and deposited in a different shape. A wide range of thermosoftening plastics can be nowadays printed, each of them has its own characteristics; the most used are[4]:

- Polylactic Acid, PLA: it is the most common FDM material, due to its low cost and ease of printing, thanks to the low melting temperature (180-220°C). It is a bioplastic, so it gets easily degraded by external agents; moreover, it is not suitable for temperature applications above 60°C because it tends to warp. It is also the most used plastic among domestic users.
- Acrylonitrile Butadiene Styrene, ABS: this thermoplastic has good characteristic such as resistance to abrasion and impact, and well behaves if it undergoes cyclical loads and temperature changes; moreover, it shows good mechanical properties. With respect to PLA, ABS is more ductile and impact-resistant, but has a lower tensile strength.

Thanks to the general advancements of the AM sector, and to several studies regarding this topic, nowadays plastics with greater properties can be extruded, multiplying the possibilities of application of 3D-printed products. These materials are called technopolymers or super-polymers, to highlight their superiority with respect to “classic” polymers, and they are appositely designed to bear high temperatures and stresses, making them suitable for sectors as aerospace and automotive, where they can even substitute metallic parts. Carbon-PEEK and ULTEM™ are two important technopolymers which will be deeply analysed in the following chapters, in which an evaluation of their tensile properties will be done.

Metals and Ceramics Metallic and ceramic parts can be printed using FDM, but some considerations must be done. In the case of metals, their melting temperature is too high to be reached by modern nozzles; as regards ceramics, they are too fragile to be stored as filaments. It means that pure metallic or ceramic FDM is impossible to be achieved, currently.

The solution that is being adopted is mixing metallic or ceramic powder with binder polymers and some additives; the filament is created and extruded. During extrusion, the plastic part melts due to the heat. At the end of this step, the resulting green part undergoes a debinding process during which the binder component flows away, and the metallic/ceramic particles fuse together. This operation is also necessary to close the pores that are present inside the structure.[22]

This process shows some difficulties, since it depends on many factors and, also, a not-so-easy sintering step is necessary: the definition of the entire procedure

must be very accurate and take into account all the different parameters, such as the ratio between polymer and filler and also the internal distribution of the powder particles. Another obstacle is determining the perfect composition of the binder polymer; a possible method is following multi-objective optimization and searching for the best combination of the variables.[23]

On the other hand, this technique offers undoubted advantages. Firstly, a general reduction of wastes with respect to “traditional” technologies: all the metallic/ceramic material is in fact used during FDM. Moreover, if compared with other AM processes based uniquely on powder (Selective Laser Sintering, Selective Laser Melting. . .), Fused Deposition Modelling reduces the costs, because the equipment is less expensive, and there are no risks associated to the use of powder (if badly handled, it could cause explosions and interfere with the human body). Some materials that can be printed in this way are Fe, steel and various alloys.[24][25]

1.3.3 Advantages and Limits of FDM

FDM shows both advantages and limitations with respect to traditional techniques and other AM processes.

Comparing FDM with other additive technologies, one of the main advantages is that it ensures good performances as regards dimensional tolerances and superficial rugosity: this means that printed parts require less post-processing operations, hence reducing time and costs. Furthermore, exploiting multi-nozzles machines, supports may be printed in a material different from the part’s one; in some cases, they can even be soluble in water, meaning that there is no risk of damaging the product while removing them; it is important to notice, however, that they can be employed only if the two materials are compatible with each other. With respect to traditional techniques, in the following paragraph will be shown that FDM allows to reduce time and costs, thanks to the relatively low price of the equipment. About this, some domestic low-cost printers exist too, but their performances cannot be compared with the one of the industrial machines; however, these smaller and more affordable tools contribute to increase the popularity of Additive Manufacturing and FDM itself among the customers. The availability of several materials and the presence of open-source software are also plus points for this technique. Finally, as said before, this technology produces minimal waste of material. Considering all these aspects, FDM is surely a competitive process, and it is in fact one of the most established AM methods in the modern industry.

Obviously, FDM presents some disadvantages and limitations. Due to the nature of the process itself, very good performances regarding accuracy and part quality are not so easy to achieve, despite being one of the most accurate AM techniques; surface roughness of FDM-printed parts is mainly influenced by the so-called “stair

stepping effect”, caused by the software during the creation of the layers: the object gets horizontally sliced and undergoes an unavoidable approximation of its external surfaces. This element causes a not perfect adhesion between two consecutive layers, enhancing high roughness values, porosity and crack formation. Hence, post-processing is very often necessary to reduce surface roughness; depending on the building material, both mechanical and chemical processes can be used, such as sanding, grinding or impregnation. This causes an increment of time and costs especially for big pieces. Then, support removal is another disadvantage, since it must be done manually, and it is not always easy: the risk of damaging the product is concrete and some little defects may remain on the surface of the piece. Again, it is a time-consuming activity in case of big, complex products. Some limitations are related to the equipment: for instance, nozzles have a certain finite resolution that prevent them to print very small details; the dimensions of the building chamber and of the platform limit how big the products can be; a single machine can print a limited range of materials.[2][26]

1.3.4 Industrial Applications and Prospects

FDM is a very versatile technique: the wide range of available materials and all the advantages related to Additive Manufacturing makes it suitable for a lot of applications. Thanks to the possibility of creating customized and detailed parts in a limited amount of time, the process is particularly suitable for creating prototypes (Rapid Prototyping); these properties can be conveniently exploited also for biomedical applications (i.e., in dentistry) and other fields in which small or medium batches of products are requested: for instance, the costs and the wastes of creating a polymeric mould are lower than building a metallic one. Also, the combination of FDM and Reverse Engineering (whose concept will be briefly described in the following lines) makes it possible to repair damaged parts even without having the original drawing. Some of the principal applications will be now described:

Rapid Prototyping (RP) Prototyping is one of the most important steps when a new product is being projected. Different types of prototypes exist and FDM technology is powerfully employed for conceptual and functional ones (actually it is the second most used AM technique, after Stereolithography). Conceptual prototypes are simply used to understand if the shape of the projected part is right and for assembly checking, so the material of the mock object is not important; so, the rapidity in obtaining the prototype has a terrific importance and AM techniques give the opportunity to obtain single, customized parts very quickly. Functional prototypes represent the following step: these must be in the same material of the ultimate part, but it doesn't matter if the technique is different, so FDM can be efficiently exploited even if

the final product won't be produced in this way. RP is mostly used in sectors such as automotive, aerospace, biomedical.[27]

Rapid Repair AM offers the possibility to repair and restore a damaged piece in an automated way, without necessarily requiring the operations of a skilled manual worker. As regards this application, FDM is not the most used AM technology, but in literature a few documents about it are present. The restoring process involves the use of Reverse Engineering (RE): by means of an optical scan, the geometry of the damaged part is obtained, and the data get elaborated to recreate the desired project, which will be then printed. This technique is advantageous especially for fields (such as marine and offshore industries, aircrafts...) for which the production of single units is very expensive and for repairing object of complex shapes. Furthermore, it is advantageous also in terms of wastes, since a broken part can be restored and reused, enhancing circular economy.[28]

Automotive This sector was one of the first in which AM techniques were employed, due to the fact that prototypes are widely used and, as already written before, FDM can be exploited for their production. Another major application in this field regards the creation of jigs, fixtures and gauges: these are useful tools needed, for example, during assembly or for checking parts. If they are made of plastic, instead of metal, they are lighter but still very durable; moreover, if they break, they can rapidly be re-printed, saving time and costs. Important manufacturers have already adopted FDM, for instance the well-known company Ford utilized more than 50 3D-printed components for building one of its cars, and BMW has used FDM for several years now, to print more ergonomic tools to be used during assembly.[29]

Aerospace Besides the production of jigs and fixtures and of prototypes, many applications in this field rely on "metal substitution": nowadays, some printable materials are characterized by high mechanical properties (similar to metals) and other useful characteristic, e.g., ULTEMTM is flame-retardant. So, heavy, metallic aircraft parts can be substituted by lighter, polymeric or composites ones, characterized by the same properties. The reduction of the structure's weight causes a lower use of fuel and a subsequent decrease of pollution. Moreover, FDM adapts particularly well to this sector since it often requires low volume productions: several case studies demonstrate that using this AM technique gives many advantages, reducing time and costs. Some applications regard helicopter's pilot sticks, parts of air supply ducts on jets and structural parts of rockets.[30][31]

Biomedical applications The medical field represents the third largest sector employing Additive Manufacturing, exploiting the possibilities of obtaining

dimensionally accurate products in a little amount of time. Moreover, FDM can be integrated with Reverse Engineering and digital scanning techniques such as CT (computed tomography) or MRI (magnetic resonance imaging), to obtain fully customized parts, based on the anatomy of the patient. Medical applications include soft scaffolds (support structures to facilitate cellular growth), blood vessels, cartilage, joints. FDM also has a certain importance in drug delivery: the availability of biocompatible materials allows the printing of tablets and other devices.[26][32]

Other applications can be individuated in moulds for injection moulding, toys sector, electronic industry, and energy storage devices, among others.[33][34]

Chapter 2

Equipment and Materials

2.1 Additive LAB at *Punch Torino S.p.A.*

This Thesis was prepared during a seven-month internship at *Punch Torino S.p.A.*, in collaboration with the Pre-Production Engineering department. The latter is in charge of the society's Additive Manufacturing Laboratory (AM Lab), consisting in four FDM printers: *Ultimaker S5 Pro Bundle*, *Markforged X7*, and *Markforged OnyxPro* since 2019, and *Roboze Argo* since May 2022; the latter is the object of this Thesis.



Figure 2.1: From left to right: *UM S5*, *MF X7*, *MF OnyxPro*

The machines principally cover internal projects, printing both prototypes and final products specially designed for useful applications inside the factory, such as particular tools for the metrology laboratory, the workshop, or the test benches; when possible, also substitutive parts of other machines get printed, and this is convenient when buying a replacement for the broken item would be very expensive. With the acquisition of *Argo 500*, more materials became available, including high performing super-polymers impossible to be printed with the rest of the equipment: this is a great opportunity to expand the AM production of *Punch*, enabling the creation of a new industrial procedure totally focused on commissions coming from external customers. In this way, the company can benefit from the printer both economically, since the activities would obviously be paid, and commercially, opening the possibility to establish a collaboration with the clients.



Figure 2.2: *Roboze Argo 500*

2.2 *Roboze Argo 500*

Roboze is an Italian company founded in Bari in 2015 and specialized in the building of FDM printers. Their machines are capable of printing super-polymers, so they can be exploited in many different sectors. As of 2022, it has more than 120 employees and has sold printers in more than 25 countries, and it has opened a second headquarter in Houston, Texas, in addition to the Apulian one.

Roboze produces two branches of machines: “Professional Series” printers, smaller machines capable of printing super-polymeric prototypes or little parts, declared to be twice as fast as other equivalent tools, and “Production Series” printers, devoted to larger parts and bigger batches.[35]

The *Argo 500* belongs to the latter category, having an available printing volume of $500 \times 500 \times 500 \text{mm}^3$, inside a chamber that can be homogeneously heated up to 180°C . The movement of the extruder and of the building platform is due to racks and pinion gears, guaranteeing more precision ($10 \mu\text{m}$ in the horizontal plane, $25 \mu\text{m}$ in the vertical direction) and repeatability with respect to “traditional” industrial printers controlled by rubber belts. To pursue the goal of metal replacement, the machine is capable of extruding super-polymeric and composite filaments at temperatures up to 450°C (in the extruder); it is currently under development the implementation of a double-nozzle technology that will make the printer able to use two different materials in the same job. The nozzles come in two configurations, “speed” and “quality”: the first is characterized by a $\text{Ø}0.6 \text{ mm}$ hole and a resolution of 0.300 mm ; the second has to be used for more detailed jobs, having a $\text{Ø}0.4 \text{ mm}$ hole, resulting in resolution equal to 0.225 mm . The machine is equipped with four dryers in which the plastics undergo a preliminary drying process, in order to get rid of moisture and improve the printing quality.

Both “traditional” and high-performance polymers can be printed, ranging from ABS, PLA, and Nylon, to PEEK, Carbon PEEK and ULTEM™. *Roboze* engineers studied accurately each of them and determined the optimal parameters and tools to be used to obtain high quality parts. In fact, each material must be extruded by a certain type of nozzle, that can be a “Tip2-B” (for unfilled, relatively low-melting materials), a “Tip2-HA” (filled, low-melting materials) or a “Tip3-HSA” (high-melting materials). Also, a different build sheet has to be applied on the platform, based on the polymer that is being used: each type of sheet has some particularities that optimize the adhesion of the first deposited layers. Moreover, important parameters have to be set or respected to obtain perfect parts: for instance, minimum amounts of time regarding the drying of the spools or the preheating of the chamber, and operating temperatures. Each information has been collected into tables to be carefully followed when using the *Argo 500*.

2.3 Materials

2.3.1 Carbon PEEK

Carbon PEEK (C-PEEK) by *Roboze* is a fibre-loaded version of the technopolymer PEEK (polyether-ether-ketone). It contains 10% short Carbon fibres, improving compression resistance, stiffness, and load capacity. It is one of the best choices as regards metal replacement, thanks to its good resistance to abrasion and wear and its

very good mechanical properties (table 2.1, considering the "xy" configuration[36]), which make it suitable also for extreme environmental conditions. Its excellent mechanical properties make it suitable for creating both functional prototypes and parts.

Properties		
Tensile Strength (25°C)	125.8	MPa
Young's Modulus (25°C)	8.1	MPa
Flexural Strength (25°C)	144	MPa
Flexural Modulus (25°C)	5.1	MPa
Shore Hardness	84.7	D scale
Melting Temperature	345	°C
Glass Transition Temperature	138	°C
Thermal Expansion Coefficient	0.00004	K ⁻¹
Specific Weight	1.33	g/cm ³
Colour	Black	

Table 2.1: Extract of the Carbon PEEK Technical Data Sheet

Many different sectors take advantage of the characteristics of Carbon fibres reinforced PEEK (the reinforcing can come in different percentages): Aerospace and Automotive exploits its low specific weight ($1.33g/cm^3$)[36] obtaining products lighter than the original ones made of steel, pursuing the idea of metal replacement[37]; it is also used, for example, in parts of vehicles' braking system[38]; Oil and Gas industries create very resistant tubes; its biocompatibility makes it usable in the Biomedical and Dental engineering[3]. Common applications also regard parts of pumps and compressors, gaskets (fig.2.3, taken from [36]), bushings.[39]



Figure 2.3: Gasket made of Carbon PEEK

For this Thesis, when working with Carbon PEEK the following parameters and instructions were always completely followed to guarantee optimal printing conditions (table 2.2), as suggested by *Roboze*:

Parameters		
Build Sheet	Translucent Beige	
Nozzle type	Tip3-HSA	
Nozzle diameter	0.6	mm
Drying time	8	hours
Drying temperature	100	°C
Chamber pre-cond. time	1.5	hours
Chamber pre-cond. temperature	160	°C
Extruder temperature	450	°C

Table 2.2: Adopted parameters for Carbon PEEK

2.3.2 ULTEM™9085

ULTEM™AM9085F by *Sabic* is a mixture of thermoplastics obtained by adding polycarbonate to a polyetherimide base. It is a technopolymer having good mechanical (table 2.3, considering the "xy" configuration[31]) and electrical properties, but most of all it is suitable for high temperature applications, since it is one of the best flame retardant materials. It resists to hydrolysis and acid solutions, and also to UV radiations and atmospheric agents.[31]

Properties		
Tensile Strength (25°C)	87	MPa
Young's Modulus (25°C)	2.6	MPa
Flexural Strength (25°C)	57	MPa
Flexural Modulus (25°C)	2.3	MPa
Melting Temperature	280	°C
Glass Transition Temperature	177	°C
Thermal Expansion Coefficient	0.000057	K ⁻¹
Specific Weight	1.27	g/cm ³
Colour	Beige	

Table 2.3: Extract of the ULTEM™Technical Data Sheet

Its characteristics makes it ideal to be used in the Aerospace industry[40]: this resin successfully satisfies international regulations, and its usage has been approved

by FAA (Federal Aviation Administration); its lightness, coupled with its physical and mechanical properties, represents a serious candidate for metal replacement. ULTEM™'s resistance to hydrocarbon, alcohols, and water solutions makes it suitable to be used in creating ducts (fig.2.4, taken from [41]) for the Automotive sector. Energetic and Petroleum industries are able to employ components for rotors, pumps, drills and sensors. Other applications regard circuit boards, eyeglasses, and equipment for food preparation and sterilization.[42]



Figure 2.4: Duct made of ULTEM™9085

As for C-PEEK, when printing with ULTEM™*Roboze's* instructions have been carefully followed to guarantee a theoretically optimal result. Table 2.4 collects the principal parameters and tools that were used.

Parameters		
Build Sheet	Translucent Dark Grey	
Nozzle type	Tip3-HSA	
Nozzle diameter	0.6	mm
Drying time	8	hours
Drying temperature	120	°C
Chamber pre-cond. time	1.5	hours
Chamber pre-cond. temperature	180	°C
Extruder temperature	380	°C

Table 2.4: Adopted parameters for ULTEM™

Chapter 3

Capability Assessment

If not differently specified, all the images, descriptions, and reference values contained in this chapter have been taken from the ISO/ASTM 52902:2019 Standard[43].

3.1 Introduction

The capability assessment[43] is a test that can be conducted on specific 3D printed specimens to investigate how precise a machine is, by creating a certain number of test pieces and measuring some of their features. The repeatability of the printer can also be studied, by making it create the same object multiple times. Moreover, the same item can be oriented differently to check that the system is able to maintain constant printing properties along both X and Y directions.

The test was done following ISO/ASTM 52902:2019 Standard, adoptable for any AM technique: it gives instructions regarding the specimens that should be printed, the features to be measured, and contains the reference drawings and values. It suggests a set of benchmarking test pieces to be built and measured, but printing all of them is not necessary and a selection can be made. Furthermore, the document describes different ways to gauge features: each method has a certain precision and, consequently, a certain reliability; based on the desired level of accuracy, a particular approach should be selected rather than another.

Some of the cases in which a capability assessment is useful are:

- Capability evaluation of an AM system: as already explained, by comparing the nominal values contained in the Standard, and the measures of the “real” piece, it can be understood if the system is working properly and evaluate its accuracy. Some benchmarks can also be defined, such as the smallest hole or the thinnest rib the printer is able to create.

- Calibration of an AM system: thanks to the comparison between nominal and real measures, it can be figured out also if the printing parameters are on point or should be changed. In the previous chapters it has already been written that the printing quality is influenced by several values, and even a small modification may influence the final results; exploiting the capability assessment tests, the optimal set of parameters can be identified, by checking which of them better reply the CAD designs.
- Performance comparison between different AM systems: printing the same test artifacts with different systems, and comparing the results, it can be defined which of them performs better. It is highly possible that a printer will be more accurate in creating certain features, while the other machine will be better for the other specimens.

For this Thesis, capability assessment tests have been conducted on all the four printers owned by *PUNCH Torino*, to elaborate a complete report about the performance of each machine. A general procedure has been established by choosing a common set of specimens to be measured, and defining fixed measurement techniques, in order to have results as comparable as possible. It must be noticed that, since the work of this Thesis regards the characterization of the *Roboze Argo 500*, the description of the capability assessment procedure will be focused on this printer, even if it has been the last to be tested (the rest of the equipment was analysed prior its installation). Moreover, an additional test has been done on it, with a set of specimens defined by *Roboze* itself (par. 3.2.1).

3.2 *Roboze Argo 500*

3.2.1 Post-installation Capability Assessment: Ultra-PLA

After the installation of the *Argo 500* in the Lab, *Roboze* asked for a capability assessment to check the performance of the newly installed machine. A preliminary test was made in Bari by *Roboze* operators, but another one was necessary to find out if some problems emerged during the transportation to Torino. Also, it was used to guarantee that the printer's performance was respecting the benchmark declared by the manufacturer. The selected material was Ultra-PLA, since it is one of the most used plastics and it does not require any time consuming pre- or post-printing operation. The nozzle was a Tip2-B (diameter $\varnothing 0.4\text{mm}$).

The company sent a G-Code (fig.3.6) ready to be used, containing seven specimens:

- 1x thickness resolution rib
- 2x resolution slot angles (parallel to X and parallel to Y axis),

- 1x circular artifact,
- 2x axis resolution artifacts (one for X, one for Y),
- 1x vertical resolution artifact (Z axis).

Some of them were taken by ISO 52902 Standard, while others were created *ad hoc* by *Roboze* engineers to check a particular feature; in the following, it will be reported if the specimen was created by them.

Thickness Resolution Rib This specimen is useful to define the precision of the machine in creating thin walls, and so the thinnest wall it can print. It consists in six ribs of different thickness, supported by quasi-oval pillars.

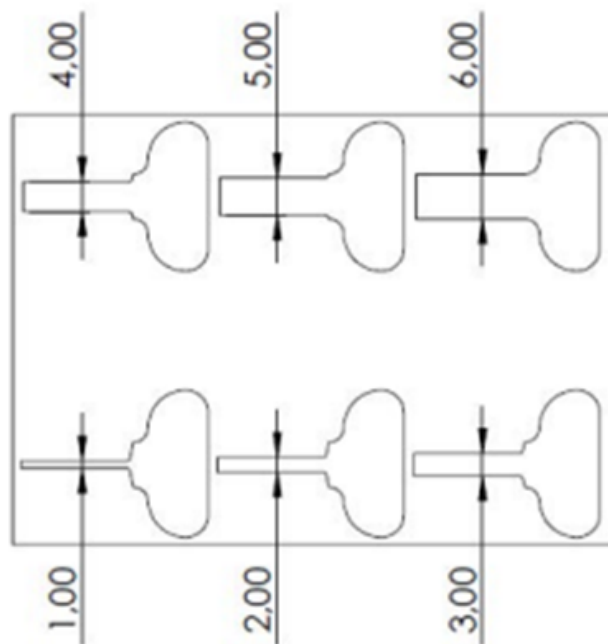


Figure 3.1: Thickness resolution ribs artifact (*Roboze*)

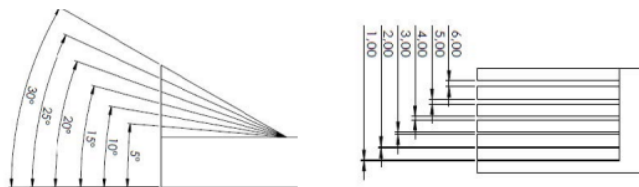


Figure 3.2: Thickness resolution slot angles artifact (*Roboze*)

Resolution Slot Angles The specimen is formed by seven branches and the features of interest are the six spacing among them: in this case, the width of each slot had to be measured. The nominal width changes through the specimen. Also, the branches are inclined with respect to the connecting branch, so the angles they form can be evaluated, in order to define an angular conformity. Two specimens were printed to test the accuracy along X and Y axes, respectively.

Circular artifact Geometrically, this artifact consists of a tear-shaped base, supporting two concentric rings of different thickness; also, a circular hole is present, in the center of the other two circumferences. By measuring each diameter, the printer's accuracy in creating concentric circles is evaluated. With respect to the circular artifact suggested by the Standard, here a $\text{Ø}15$ diameter is present instead of a $\text{Ø}16$.

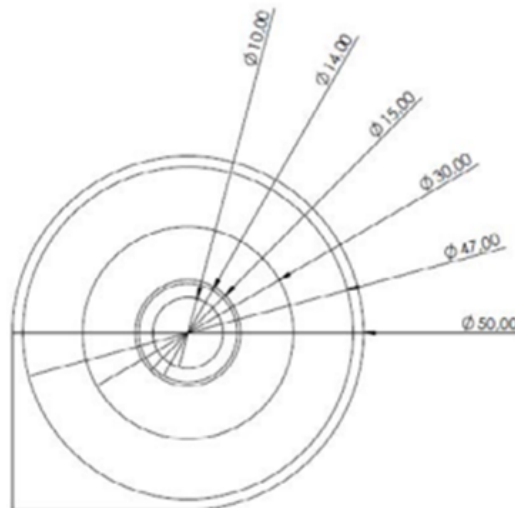


Figure 3.3: Circular artifact (*Roboze*)

Resolution X/Y axis artifact This artifact is very similar to the linear artifact proposed by ISO 52902. A slim rectangular base supports five prismatic protrusions; the distance between them is not constant. Both the size of the prisms and the spacing among them are measured, to check the linear positioning accuracy of the machine along a certain direction, and the repeatability regarding the creation of the same protrusion in different points of the plate. Two identical artifacts were printed, the one parallel to X axis, the other to Y axis.

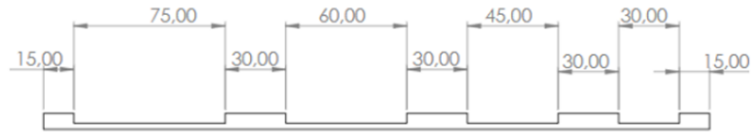


Figure 3.4: Resolution X/Y axis artifact (*Roboze*)

Vertical Resolution Z axis artifact This artifact is not included in the ISO Standard but was projected by Roboze in order to evaluate the capability of the printer to create features on a high vertical wall. In this way the perpendicularity of the vertical face can be studied, too. The distance between the different “steps” is equal to 40 mm.

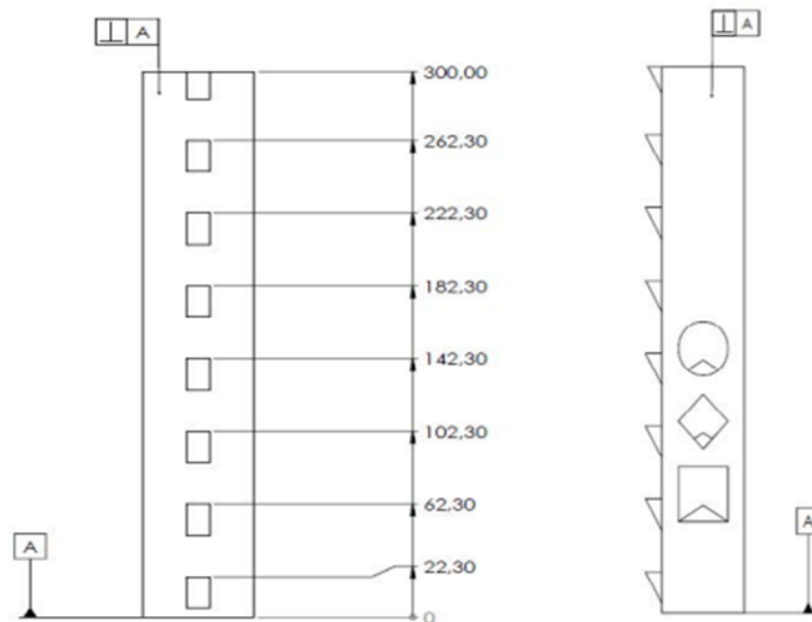


Figure 3.5: Vertical resolution Z axis artifact (*Roboze*)

Roboze also provided a file containing all the reference drawings and values, requirements about how to measure each feature (the tool and the procedure to follow), and the tolerance values to check the conformity of all the pieces; with regard to this latter element, a piece was considered to be “not conform” if at least one of the measures relative to it was out of tolerance. The measurements of this set of specimens were taken by a Metrology Lab operator in *PUNCH Torino*, since some instruments (e.g., the CMM) require a qualified user to utilize them. It must be

said that each artifact could have been exploited to investigate other aspects of the *Argo*'s performance, but the measurements have been limited to the requests of *Roboze*.

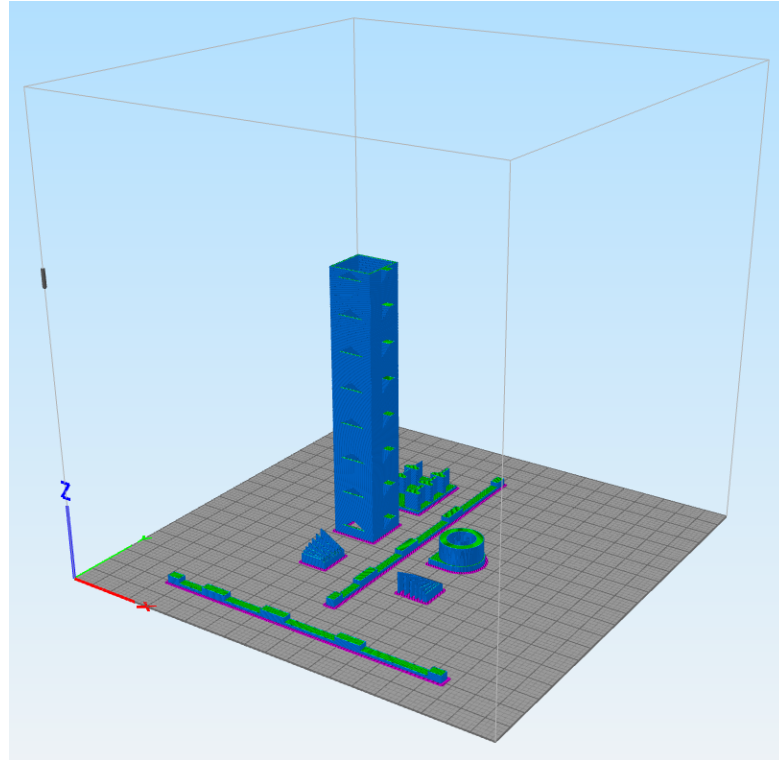


Figure 3.6: PLA: buildsheet preparation on *Simplify 3D*

3.2.2 Results and Analysis

The tables contain the results of the measurements, along with the reference values and tolerances to be respected. The order is the same as the list in paragraph 3.2.1. Analysing the results, the following aspects can be highlighted:

- Apart from one value related to the circular artifact ($\text{Ø}14$), all the measured features are in tolerance; this means that all the specimens are conform (apart from the previously cited one).
- With regards the circular artifact, after a discussion meeting with *Roboze*, it is considered conform: the out-of-tolerance value is in fact due to the resolution of the nozzle. The internal ring is 0.5 mm thick, a value that is physically impossible to achieve with a $\text{Ø}0.4$ mm nozzle. Indeed, the machine creates a first circumference, whose thickness is approximately 0.4 mm; after detecting

that 0.4 is less than 0.5 (which is the nominal thickness value), it creates another circle next to the other: its width becomes $0.4 \times 2 = 0.8mm$, overcoming the reference value. It is easy to understand that either printing only one circle, or printing two circles, one diameter will be always not compliant.

- The effectively employed tools were not always the ones that were suggested. In some cases, this shift has been done in order to obtain more precise measurements (e.g., when the CMM was used instead of a caliber), giving more reliability to the results. Instead, two instrument changings regarded the resolution slot specimens: to measure the inclination of the branches, the CMM was employed in place of the goniometer, since the latter was impossible to be used due to the presence of the connecting arm; to measure the width of the slots a caliber was utilized, because the Johnson blocks would have deformed the branches, altering the real spacing. The measure was taken at the bottom of the slot, where the features are stiffer.
- To sum up, considering that all the measures are conform (the only non-conformity is related to mechanical limits), the printer does not present any problem and satisfy all the requirements.

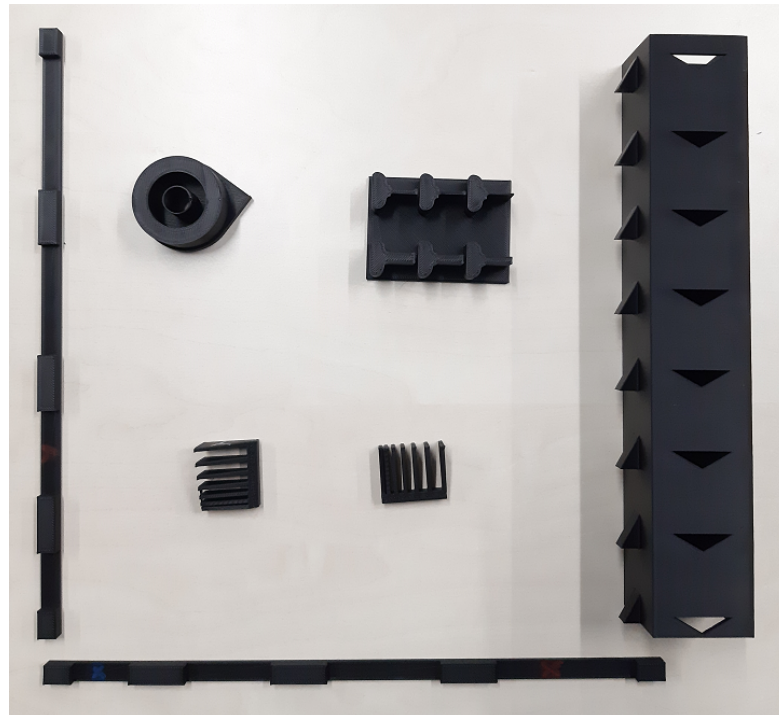


Figure 3.7: PLA: printed pieces

The same set of specimens (fig.3.7) will be printed and tested regularly, to check the machine continues to fulfil the tolerance values and guarantees constant properties; the results will be periodically transmitted to *Roboze*. Also, the test may be repeated with different materials.

Thickness Resolution Ribs artifact		
Feature	Nominal (mm)	Measured (mm)
Rib thickness	1.0	1.02
	2.0	2.02
	3.0	3.02
	4.0	4.00
	5.0	4.99
	6.0	6.01

Table 3.1: PLA: thickness resolution ribs artifact

Resolution Slotted Angles (X)		
Feature	Nominal	Measured
Branch inclination	5°	4.93°
	10°	9.67°
	15°	14.81°
	20°	19.73°
	25°	24.67°
	30°	29.63°
Slot width	1.00 mm	1.05 mm
	2.00 mm	2.03 mm
	3.00 mm	3.04 mm
	4.00 mm	4.00 mm
	5.00 mm	5.02 mm
	6.00 mm	6.01 mm

Table 3.2: PLA: resolution slotted angles artifact - X axis

Resolution Slotted Angles (Y)		
Feature	Nominal	Measured
Branch inclination	5°	4.90°
	10°	9.82°
	15°	14.80°
	20°	19.77°
	25°	24.76°
	30°	29.68°
Slot width	1.00 mm	1.06 mm
	2.00 mm	2.01 mm
	3.00 mm	3.02 mm
	4.00 mm	4.01 mm
	5.00 mm	4.98 mm
	6.00 mm	6.00 mm

Table 3.3: PLA: resolution slotted angles artifact - Y axis

Circular artifact				
Feature	Nom (mm)	Meas (mm)	Feature	Meas (mm)
Diameter	10.0	9.973	Roundness 10	0.178
	14.0	13.549	Roundness 14	0.151
	15.0	15.242	Roundness 15	0.073
	30.0	29.922	Roundness 30	0.071
	47.0	46.946	Roundness 47	0.063
	50.0	49.894	Roundness 50	0.034

Table 3.4: PLA: circular artifact

X-axis Resolution artifact		
Feature	Nominal (mm)	Measured (mm)
Protrusion	15	14.98
	30	29.95
	30	29.95
	30	29.95
	15	14.96
Spacing	75	74.93
	60	60.07
	45	44.97
	30	29.98

Table 3.5: PLA: X-axis resolution artifact

Y-axis Resolution artifact		
Feature	Nominal (mm)	Measured (mm)
Protrusion	15	14.93
	30	29.90
	30	29.95
	30	29.95
	15	14.96
Spacing	75	74.96
	60	59.91
	45	44.94
	30	29.98

Table 3.6: PLA: Y-axis resolution artifact

Vertical Resolution artifact		
Feature	Nominal (mm)	Measured (mm)
Height	22.3	22.295
	62.3	62.262
	102.3	102.285
	142.3	142.310
	182.3	182.115
	222.3	222.150
	262.3	262.160
	300.0	299.760
Perpendicularity 1		0.135
Perpendicularity 2		0.211

Table 3.7: PLA: vertical resolution artifact

3.3 Capability Assessment for comparison between different materials

As written at the beginning of this chapter, the capability assessment can be used to compare the performances of different printers and understand which one should give better results in creating a particular feature. *PUNCH Torino* engineers defined a set of artifacts, taken by ISO/ASTM 52902 Standard, for two purposes: to understand if (and how much) *Roboze's* performance changes when the material changes, and to make a comparison between the four different printers. A total of seven tests have been conducted as of October 2022. Table 3.8 contains a summary

of them:

n°	Printer	Material
1	Markforged X7	Onyx
2	Markforged OnyxPro	Onyx
3	Ultimaker S5	PLA
4	Roboze Argo 500	ULTEM™9085
5		Carbon-PEEK
6		Ultra-PLA
7		Carbon-PA

Table 3.8: Recap of capability assessments

A selection of artifacts was made, for a total of 14 different parts. In reality, many of them are characterized by the same shapes, but they are scaled: in fact, different sizes of the same item can be printed: from the biggest to the smallest, coarse, medium and fine. The following list contains all the specimens and their sizes:

- 1x linear artifact, LA;
- 2x circular artifact, CA-M/F (medium and fine sizes);
- 2x resolution pins, RP-C/M (coarse and medium sizes);
- 2x resolution holes, RH-C/M (coarse and medium sizes);
- 2x resolution ribs, RR-C/M (coarse and medium sizes);
- 2x resolution slots, RS-C/M (coarse and medium sizes);
- 2x resolution slotted angles, RSA-C/M (coarse and medium sizes);
- 1x surface texture artifact, ST-M (medium size).

LA and CA specimens were chosen to investigate the accuracy of the printers, ST-M to obtain information about the rugosity of inclined surfaces, the remaining ones to study the resolution in creating various features.

Linear artifact It is the analogue of the linear artifact projected by *Roboze*, but in this case the design suggested in the Standard was used. The length of each protrusion and the distances among them were measured to evaluate the accuracy and the repeatability of the printer. Since only one LA was printed, only one direction's resolution could be verified.

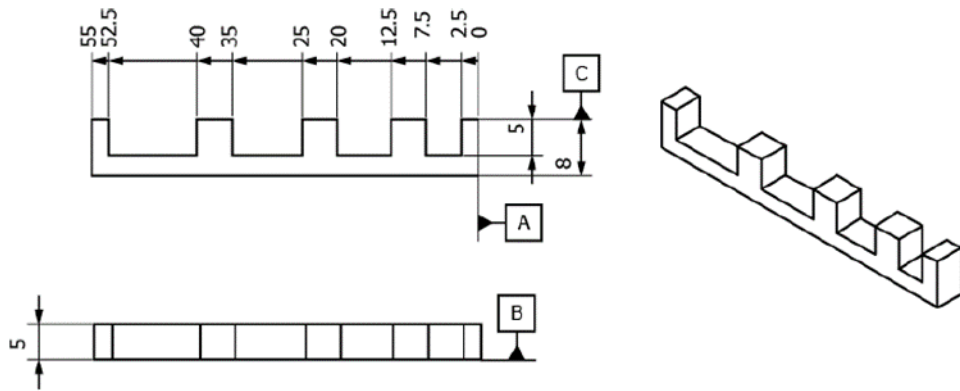


Figure 3.8: Linear artifact

Circular artifacts As for the corresponding *Roboze* version, their features of interest were the rings and the central hole; the measure of each diameter helped to check the accuracy of the system. The specimen was printed in two different sizes, to cover a wider range of values. Differently from the previous capability assessment, the designs corresponded completely to the ones contained in ISO 52902.

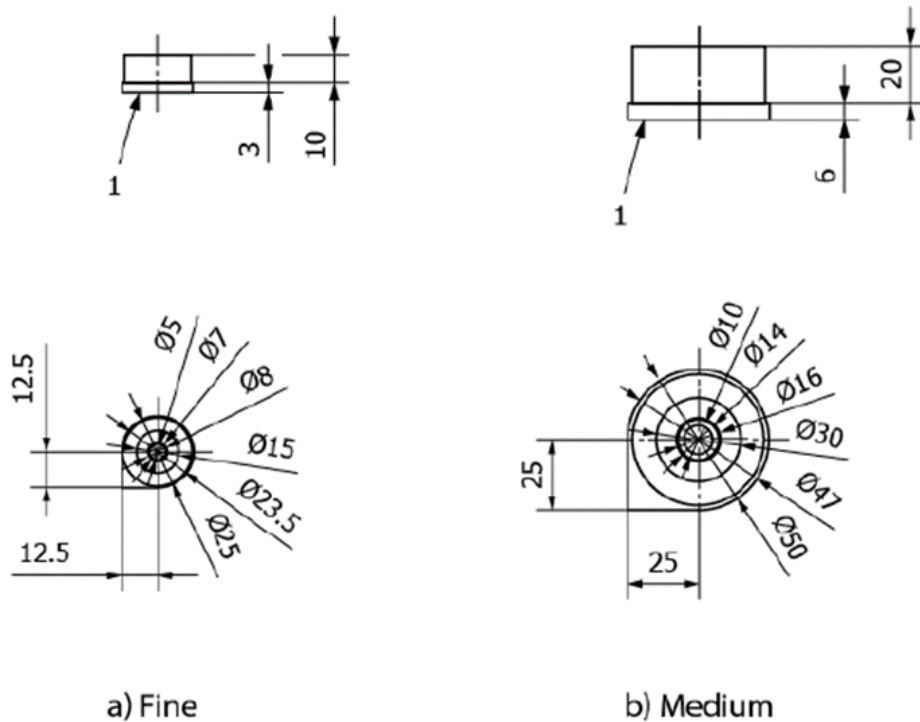


Figure 3.9: Circular artifacts

Resolution Pins artifacts These artifacts were used to define how precisely the machine creates slim features and also the smallest printable pin, by measuring its diameter. They consisted in a parallelepipedal base on which five pins were built; the selected ratio between their height and diameter was 6:1 and two specimen sizes were chosen: coarse and medium.

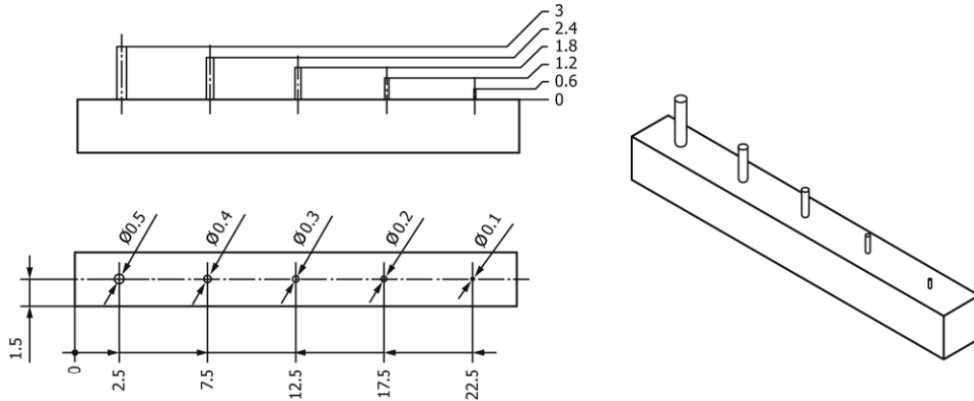


Figure 3.10: Resolution pins artifact (medium size)

Resolution Holes artifacts To check the smallest printable hole, this kind of specimen had to be used. Five holes characterized by different diameters were created on a parallelepipedal base; again, coarse and medium size artifacts were printed to investigate the results for a higher number of features.

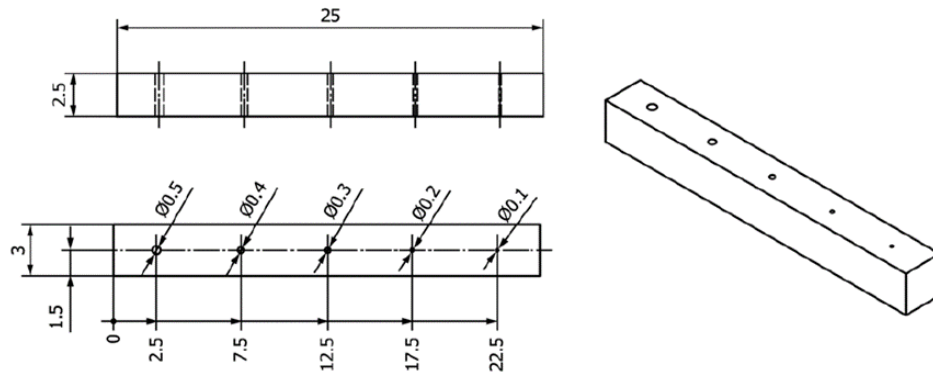


Figure 3.11: Resolution holes artifact (medium size)

Resolution Ribs artifacts It was the same artifact as in the previous capability assessment. The only differences were the shape of the pillars sustaining the ribs, which now were square-shaped, and that two different sizes were printed

(coarse and medium). The height of the ribs was 10 mm (a 20 mm option was also available).

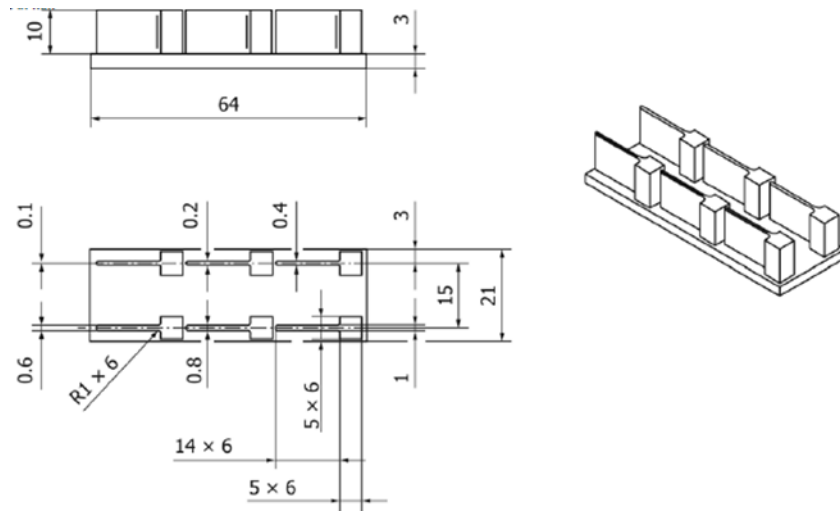


Figure 3.12: Resolution ribs artifact (medium size)

Resolution Slots-Resolution Slotted Angles artifacts These artifacts were used to define the accuracy of the printer in creating slots of a certain size, between two branches. RSA specimens had inclined surfaces. Coarse and medium sizes were selected, for a total of four items, having six slots each. The height was 10 mm.

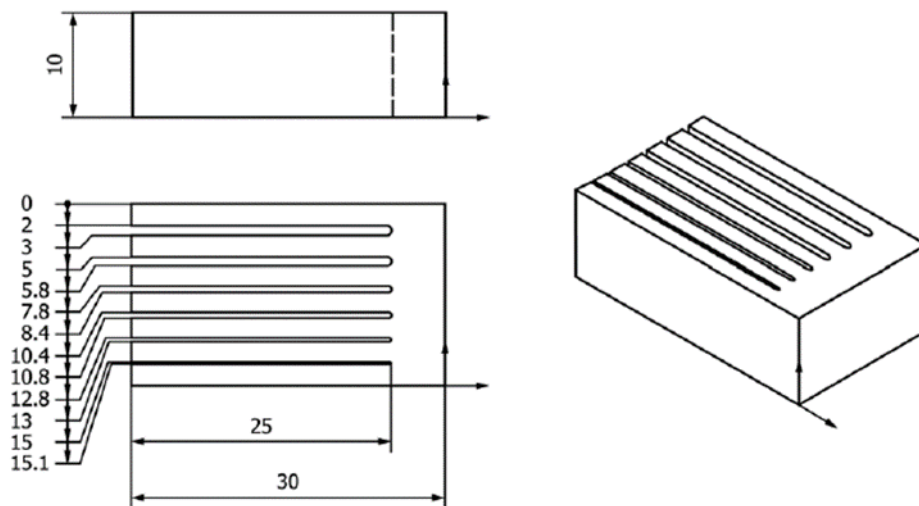


Figure 3.13: Resolution slots artifact (medium size)

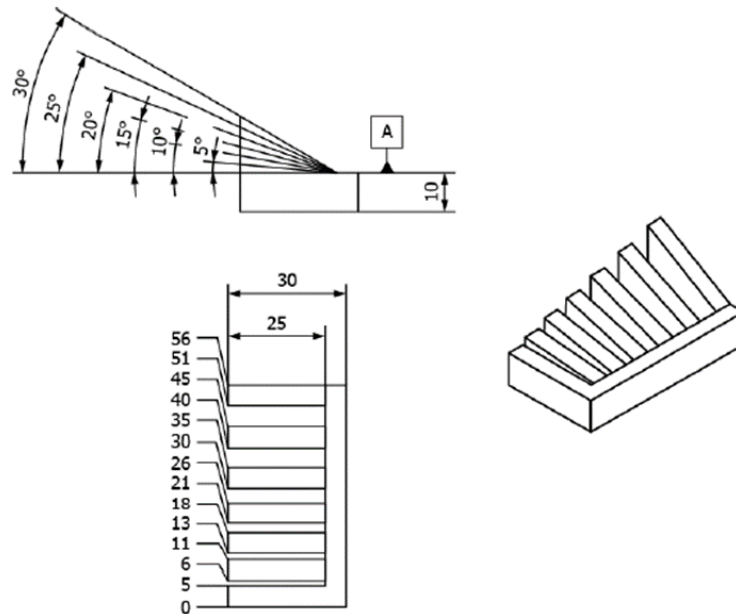


Figure 3.14: Resolution slotted angles artifact (coarse size)

Surface Texture artifact This artifact consisted in a series of seven flat tabs connected by struts, each of them characterized by a different inclination with respect to the horizontal plane from 0° to 90° . The rugosity of each surface was then measured. It was an interesting specimen because it clearly gave hints about the dimensional tolerances that can be achieved by using a certain AM technique. For a medium size artifact, the tabs measured $12.0 \times 30.0 \times 3.0\text{mm}$.

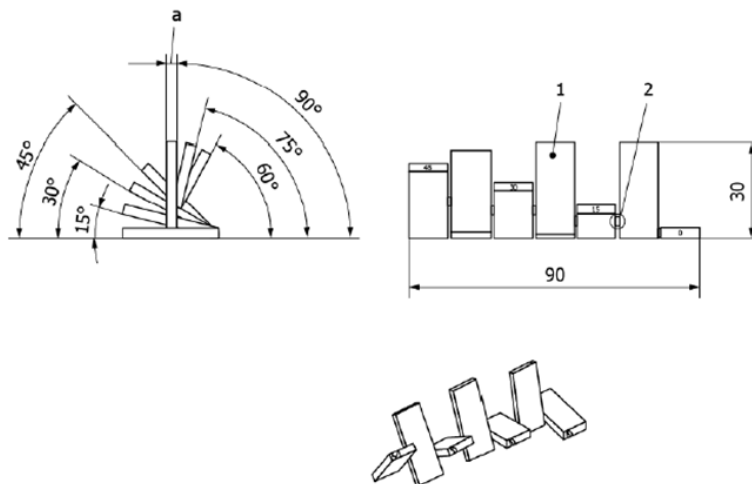


Figure 3.15: Surface texture artifact

The features that have been measured and the corresponding measuring technique/tool are contained in table 3.9; when possible, the usage of simple instruments (like calipers and feeler gauges) was privileged for two reasons: they can be used by anyone, without needing particular skills, and they are always immediately available. The measurements will obviously be less precise but can be done as soon as the print job finishes; a greater usage of more complex equipment would require a longer time before having any result, meaning the printer cannot be used in the meantime (or if it is used, its performance would not be guaranteed).

Specimen	Feature	Measuring tool
LA	Protrusion thickness Spacing	Handheld caliper
CA	Diameter	Handheld caliper
RP	Pin diameter	Handheld caliper
RH	Hole diameter	Handheld caliper CMM for smaller holes
RR	Rib thickness	Handheld caliper
RS	Slot width	Handheld caliper Feeler gauge for smaller slots
RSA	Slot width	Handheld caliper Feeler gauge for smaller slots
ST	Surface rugosity	Profilometer

Table 3.9: Measured features and tools

3.3.1 Capability Assessment: ULTEM™ and Carbon-PEEK

The following tables contain the results of the measurements of the specimens made of ULTEM™. In most cases, results were obtained by making an arithmetical average of multiple values: only for this first material, all the measures will be reported; then, for C-PEEK and all the other printers/materials, only the final results will be shown either in this chapter, or in Appendix A.

ULTEM™

ULTEM™ specimens were printed using a Tip3-HSA nozzle (diameter: 0.6 mm), whose extruder is made of a high-strength alloy capable of bearing materials characterized by high melting temperatures. As requested by ISO 52902, all the

items were printed in a single job (fig.3.16), and the most important parameters are the same listed into table 2.4.

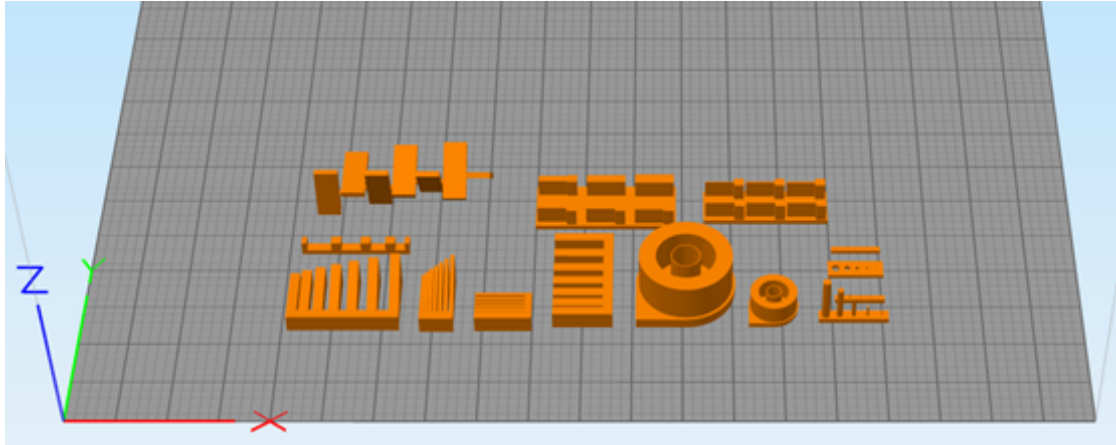


Figure 3.16: ULTEM™: preparation of the job on *Simplify 3D*

Linear artifact Three measures were taken using a handheld digital caliper, at bottom, centre and top of each protrusion; the values were then averaged.

Linear Artifact					
Feature	Nominal (mm)	Average (mm)	Bottom	Centre	Top
Protrusions	2.5	2.87	3.00	2.72	2.90
	5	5.29	5.27	5.32	5.29
	5	5.25	5.28	5.22	5.24
	5	5.35	5.40	5.39	5.25
	2.5	3.01	2.98	3.01	3.04
Spacings	5	4.69	4.70	4.79	4.59
	7.5	7.32	7.27	7.37	7.32
	10	9.74	9.75	9.67	9.81
	12.5	11.85	11.87	11.85	11.84

Table 3.10: ULTEM™: linear artifact

It can be noticed that all the protrusions are bigger than their nominal dimensions; as a consequence, all the spacings are smaller. Considering the repeatability of the printer, the three 5-mm-features are similar; the second 2.5-mm-protrusion is the worst one, being 20% bigger than its CAD version.

Circular artifacts For each diameter, two measurements are done at two different

heights: 0.25F and 0.75F, where F is the height of each ring. The chosen instrument was the handheld caliper.

Circular Artifact - medium				
Feature	Nominal (mm)	Average (mm)	0.25 F	0.75 F
Diameter	10	9.89	9.91	9.86
	14	fail		
	16	fail		
	30	29.47	29.45	29.49
	47	46.63	46.66	46.60
	50	49.62	49.65	49.58

Table 3.11: ULTEM™: circular artifact - medium size

Circular Artifact - fine				
Feature	Nominal (mm)	Average (mm)	0.25 F	0.75 F
Diameter	5	4.79	4.85	4.72
	7	fail		
	8	fail		
	15	14.77	14.75	14.78
	23.5	23.27	23.25	23.28
	25	24.76	24.74	24.77

Table 3.12: ULTEM™: circular artifact - fine size

Two diameters were impossible to be measured because the resolution of the printer is not high enough to create too thin rings. All the acquired measures are lower than the corresponding design ones.

Resolution Pins artifacts Each pin's diameter is evaluated by using a caliper and averaging three measures, taken at bottom, centre and top of the features.

Resolution Pins artifact - coarse					
Feature	Nominal (mm)	Average (mm)	Bottom	Center	Top
Pin diameter	4	4.06	4.06	4.15	3.97
	3	2.89	2.77	2.76	3.15
	2	2.22	2.32	2.25	2.10
	1	1.23	1.24	1.17	1.28
	0.5	fail			

Table 3.13: ULTEM™: resolution pins artifact - coarse size

Resolution Pins artifact - medium		
Feature	Nominal (mm)	Average (mm)
Pin diameter	0.5	fail
	0.4	fail
	0.3	fail
	0.2	fail
	0.1	fail

Table 3.14: ULTEM™: resolution pins artifact - medium size

If bigger pins are more or less precise, smaller ones were not even printed, setting an inferior threshold. Moreover, it can be noticed that the diameter of each feature varies depending on the height the measure corresponds to.

Resolution Holes artifacts Since the holes were too small to be measured with a caliper, their diameters were evaluated by means of the CMM (Coordinate Measuring Machine), averaging two measures taken at different heights with respect to the base plane (0.8mm and 1mm).

Resolution Holes artifact - coarse				
Feature	Nominal (mm)	Average (mm)	0.8 mm	1 mm
Hole diameter	4	3.52	3.55	3.49
	3	2.25	2.25	2.25
	2	fail		
	1	fail		
	0.5	fail		

Table 3.15: ULTEM™: resolution holes artifact - coarse size

Resolution Holes artifact - medium				
Feature	Nominal (mm)	Average (mm)	0.8 mm	1 mm
Hole diameter	0.5	fail		
	0.4	fail		
	0.3	fail		
	0.2	fail		
	0.1	fail		

Table 3.16: ULTEM™: resolution holes artifact - medium size

All the holes result much smaller than the virtual ones, also due to a not perfect circular shape of the features; holes whose nominal diameter was minor

than 3 mm were not even printed (RH-medium artifact was, in fact, totally failed).

Resolution Ribs artifacts The results were the average of three measures, taken in three different points of each rib with a caliper.

Resolution Ribs artifact - coarse					
Feature	Nominal (mm)	Average (mm)	Left	Centre	Right
Rib thickness	6	6.04	6.02	6.00	6.09
	5	4.97	4.97	4.97	4.97
	4	3.99	3.94	3.99	4.04
	3	3.08	3.1	3.06	3.08
	2	2.02	1.98	2.03	2.06
	1	1.29	1.24	1.31	1.33

Table 3.17: ULTEM™: resolution ribs artifact - coarse size

Resolution Ribs artifact - medium					
Feature	Nominal (mm)	Average (mm)	Left	Centre	Right
Rib thickness	1	1.31	1.27	1.33	1.34
	0.8	1.34	1.32	1.35	1.36
	0.6	fail			
	0.4	fail			
	0.2	fail			
	0.1	fail			

Table 3.18: ULTEM™: resolution ribs artifact - medium size

Again, thinner features were impossible to be created. Ribs whose nominal thickness is between 2 and 6 mm are very precise; on the contrary, 0.8- and 1-mm features are quite bigger than the respective CAD design. It can also be highlighted that the thickness of each rib does not appear to be constant along the wall length, but it varies.

Resolution Slots Two instruments were used for these specimens. When possible, the width of each slot was calculated averaging three measures (bottom, centre, top) evaluated with a caliper; otherwise, feeler gauges were used for narrower slots.

Resolution Slots artifact - coarse					
Feature	Nominal (mm)	Average (mm)	Left	Centre	Right
Slot width	6	5.92	5.91	5.92	5.92
	5	4.94	4.9	4.93	4.99
	4	3.96	3.94	3.93	4.00
	3	2.96	2.98	2.95	2.95
	2	1.99	2.01	1.96	2.01
	1	1 (feeler gauge)			

Table 3.19: ULTEM™: resolution slots artifact - coarse size

Resolution Slots artifact - medium		
Feature	Nominal (mm)	Measure (mm)
Slot width (feeler gauge)	1	1
	0.8	0.8
	0.6	0.6
	0.4	0.4
	0.2	fail
	0.1	fail

Table 3.20: ULTEM™: resolution slots artifact - medium size

These artifacts are really good: many real features are very close to the virtual ones. Without considering the failed geometries, smaller slots are exactly as wide as desired; however, it must be taken into account that their measurement was done using a feeler gauge, so possible deviations from the design cannot be detected.

Resolution Slotted Angles artifacts The same considerations for the previous artifacts can be made.

Resolution Slotted Angles artifact - coarse					
Feature	Nominal (mm)	Average (mm)	Bottom	Centre	Top
Slot width	6	5.83	5.85	5.77	5.88
	5	4.93	4.94	4.91	4.95
	4	3.97	3.93	3.96	4.02
	3	2.97	2.97	2.92	3.02
	2	1.99	1.97	1.97	2.02
	1	1 (feeler gauge)			

Table 3.21: ULTEM™: resolution slotted angles artifact - coarse size

Resolution Slotted Angles artifact - medium		
Feature	Nominal (mm)	Measure (mm)
Slot width (feeler gauge)	1	1
	0.8	0.8
	0.6	0.6
	0.4	0.4
	0.2	fail
	0.1	fail

Table 3.22: ULTEM™: resolution slotted angles artifact - medium size

The results are again really good, without considering the failed features; in fact, the obtained slots exactly correspond to their virtual version.

Surface Texture artifact The average rugosity of each surface is evaluated using a profilometer.

Surface Texture artifact - medium		
Feature	Tab inclination	Average rugosity (μm)
Rugosity	0°	15.63
	15°	16.50
	30°	16.98
	45°	22.32
	60°	38.38
	75°	23.09
	90°	9.18

Table 3.23: ULTEM™: surface texture artifact - medium size

There are no reference values to evaluate the rugosity of the tabs. It can be seen that, generally, the roughness increases as the inclination of the face increases, with the exception of the last two tabs. The rugosity is influenced by the layer height, as well as by the slicing of the CAD model: in fact, the 90° face is characterized by the lower roughness since it is perfectly perpendicular to the Z-axis.

Carbon PEEK

Carbon PEEK specimens (fig.3.17) were printed using a Tip3-HSA nozzle (diameter: $\varnothing 0.6$ mm), different from the one used for ULTEM™, in order to avoid problems such as the clogging of the extruder. The most important printing parameters are the same listed into table 2.2. Evaluating the result of the previous capability assessment, it was decided not to print two specimens: Resolution Pins and Resolution Holes artifacts (medium size). The other items and the measuring instruments were the same as before.



Figure 3.17: Carbon PEEK: specimens of the capability assessment

Linear artifact With respect to the ULTEM™specimen, the Carbon PEEK part is more precise as regards the creation of the spacings, but slightly worse in printing the protrusions.

Linear artifact		
Feature	Nominal (mm)	Average (mm)
Protrusions	2.5	2.95
	5	5.31
	5	5.20
	5	5.35
	2.5	2.84
Spacings	5	4.75
	7.5	7.34
	10	9.73
	12.5	12.21

Table 3.24: Carbon PEEK: linear artifact

Circular artifacts Numerically speaking, Carbon PEEK is more precise than

ULTEM™ for 5 measures out of 8. However, Ø5, 25 and 50 circles are very different from the virtual model, so it is impossible to clearly define which material is better than the other.

Circular artifact - medium		
Feature	Nominal (mm)	Average (mm)
Diameter	10	9.88
	14	fail
	16	fail
	30	29.84
	47	46.78
	50	48.09

Table 3.25: Carbon PEEK: circular artifact - medium size

Circular artifact - fine		
Feature	Nominal (mm)	Average (mm)
Diameter	5	4.51
	7	fail
	8	fail
	15	14.80
	23.5	23.36
	25	24.63

Table 3.26: Carbon PEEK: circular artifact - fine size

Resolution Pins artifacts In this case, the printer was able to create almost all the pins, but their quality was too bad to allow a proper measuring of their diameters.

Resolution Pins artifact - coarse		
Feature	Nominal (mm)	Average (mm)
Pin diameter	4	fail
	3	fail
	2	fail
	1	fail
	0.5	fail

Table 3.27: Carbon PEEK: resolution pins artifact - coarse size

Resolution Holes artifact Again, all the measurable holes are much smaller

than the nominal ones but are slightly better than the corresponding feature in ULTEM™. Moreover, the measurement process was not so easy due to the low quality of the holes' internal surfaces.

Resolution Holes artifact - coarse		
Feature	Nominal (mm)	Average (mm)
Hole diameter	4	3.53
	3	2.33
	2	fail
	1	fail
	0.5	fail

Table 3.28: Carbon PEEK: resolution holes artifact - coarse size

Resolution Ribs artifacts Thicker ribs are quite precise, but not as much as the ULTEM™ ones. As before, thinner ribs (1- and 0.8-mm wide) turn out to be bigger than the corresponding design, so a lower benchmark as regards these features can be set. Very thin parts were not even printed.

Resolution Ribs artifact - coarse		
Feature	Nominal (mm)	Average (mm)
Rib thickness	6	6.15
	5	5.11
	4	3.99
	3	3.12
	2	2.02
	1	1.48

Table 3.29: Carbon PEEK: resolution ribs artifact - coarse size

Resolution Ribs artifact - medium		
Feature	Nominal (mm)	Average (mm)
Rib thickness	1	1.49
	0.8	1.43
	0.6	fail
	0.4	fail
	0.2	fail
	0.1	fail

Table 3.30: Carbon PEEK: resolution ribs artifact - medium size

Resolution Slots artifacts Compared with the ULTEMTMones, Carbon PEEK artifacts are less precise, and all the slots are a lot smaller than the corresponding reference design. The medium specimen is a little better, but not as good as the ULTEMTMone. It is interesting to notice that the 1-mm slots are quite different even if the nominal width was the same.

Resolution Slots artifact - coarse		
Feature	Nominal (mm)	Average (mm)
Slot width	6	5.61
	5	4.65
	4	3.65
	3	2.73
	2	1.79
	1	0.6 (feeler gauge)

Table 3.31: Carbon PEEK: resolution slots artifact - coarse size

Resolution Slots artifact - medium		
Feature	Nominal (mm)	Average (mm)
Slot width (feeler gauge)	1	0.9
	0.8	0.8
	0.6	0.6
	0.4	0.3
	0.2	fail
	0.1	fail

Table 3.32: Carbon PEEK: resolution slots artifact - medium size

Resolution Slotted Angles artifacts Also with regard to RSA specimens, Carbon PEEK artifacts are worse than the others; actually, the medium sized specimen was not measurable at all since no slots were completely open to allow the passage of the feeler gauge. Interestingly, the 2-mm feature is bigger than the design one.

Resolution Slotted Angles artifact - coarse		
Feature	Nominal (mm)	Average (mm)
Slot width	6	5.66
	5	4.72
	4	3.74
	3	2.88
	2	2.05
	1	0.6 (feeler gauge)

Table 3.33: Carbon PEEK: resolution slotted angles artifact - coarse size

Resolution Slotted Angles artifact - medium		
Feature	Nominal (mm)	Average (mm)
Slot width (feeler gauge)	1	fail
	0.8	fail
	0.6	fail
	0.4	fail
	0.2	fail
	0.1	fail

Table 3.34: Carbon PEEK: resolution slotted angles artifact - medium size

Surface Texture artifact As before, the average rugosity increases as the inclination of the tab grows. The 90°-face is the less rough for the same reasons previously explained. Comparing the results of both the materials, Carbon PEEK is generally better than ULTEM™, except for the 30° and 75° faces, that are slightly rougher.

Surface Texture artifact - medium		
Feature	Tab inclination	Average rugosity (μm)
Rugosity	0°	15.57
	15°	16.15
	30°	19.51
	45°	19.98
	60°	24.16
	75°	24.78
	90°	4.96

Table 3.35: Carbon PEEK: surface texture artifact - medium size

3.3.2 Results and Analysis

The following table (table 3.36) contains final considerations about the results of the capability assessments just described.

Specimen(s)	Comments
Linear artifact	The best choice is not clearly identifiable; protrusions are better made by ULTEM™, while spacings are more precise in the C-PEEK specimen.
Circular artifacts	Any of the materials is significantly better than the other. The ULTEM™specimens are characterized by more precision in creating the smallest and the largest diameters of each part, while C-PEEK ones give better results for the intermediate circles. The machine was not able to print the thinnest internal ring of each artifact.
Resolution Pins artifacts	Considering exclusively the coarse-size artifact, ULTEM™is clearly better even if the results are not so good. C-PEEK specimen is characterized by a very low quality that made the measuring impossible. Also, the smallest pins were not printed.
Resolution Holes artifacts	All the holes were smaller than the nominal ones, and C-PEEK performs slightly better. RH-fine artifact was completely failed by ULTEM™, so it was not printed in C-PEEK.
Resolution Ribs artifacts	ULTEM™specimens are generally better than C-PEEK ones; however, 1-mm and 0.8-mm ribs are dimensionally unacceptable due to the big difference from the nominal values. Thinner ribs could not be printed.
Resolution Slots artifacts	Both the ULTEM™specimens are very good, the smaller slots perfectly reply the virtual part; C-PEEK gives worse results.
Resolution Slotted Angles artifacts	Again, ULTEM™artifacts are almost perfect, with real measures very close to the CAD design. On the contrary, C-PEEK parts are not good, especially the medium-size one that completely failed (no slots were measurable).
Surface Texture artifact	In both specimens, the average surface roughness increases as the inclination of the tabs grows; this trend does not apply only for the 75° face of the ULTEM™artifact. The least rough tabs are the 90° ones, since they are perpendicular to the Z axis and so they are not affected negatively by the slicing operations. C-PEEK is generally better than ULTEM™.

Table 3.36: Comparison between ULTEM™and Carbon PEEK - capability assessments

To conclude, these tests were useful to set benchmarks regarding the machine’s capability. As expected, very small features were impossible to be printed, or their quality was not good enough: this is principally related to the nozzles, which inevitably have some technological limits due to their limited resolution. It would be interesting to repeat the test using a smaller nozzle (e.g., with a diameter of 0.4 mm), and compare the results. However, the printer managed to create all the bigger features, even if it is clear that some of them were not perfect: this aspect should be taken into account when projecting using these materials and consider if it would be necessary to slightly oversize (or undersize) the element to respect the desired dimensions. The fact that the printer failed the creation of some artifacts is not a major problem, since the capability assessment aims to define limits on its usage. It may be useful to repeat the tests periodically to control the maintenance

of the printer's performance, otherwise it may be done whenever the nozzle changes or after a long no-printing period of the machine.

Chapter 4

Tensile Tests

4.1 Introduction

After the characterization of the machine's performance, to better understand the behaviour of ULTEM™ and Carbon PEEK, several tensile tests were conducted. It was decided to perform these tests for various reasons: first of all, knowing the real mechanical limits of the materials allows to project functioning parts, without risking their failure; this aspect contributes to increase the reliability of the company with its customers, since *Punch* will be able to guarantee that the products will satisfy the external requests. Moreover, the obtained results will contribute to extending the scientific knowledge about the usage of the involved materials and the FDM technology, especially considering that it is an anisotropic process affected by several parameters (cfr. chapter 1.3.1).

The scope of this thesis was to understand how and how much different parameters influence the mechanical properties of the printed parts. It is clearly impossible to study the impact of each parameter all at once, so a selection of a restricted number of variables had to be made.

4.1.1 Parameters

Other than considering two different materials, ULTEM™ and Carbon PEEK, the final selection included three other parameters: printing orientation, infill rate and testing temperature.

- Printing orientation: this parameter represents the orientation of the part with respect to the three principal axes; the direction of each axis is shown in fig.4.1, left, coherently with the printer's set up. Two alternatives were chosen, namely *xy* (horizontal or flat) and *zx* (vertical or upright): the letters stand for the directions of the two principal dimensions of the part. The choice

depended on the fact that these two orientations seems to be the benchmarks of many tensile tests performed on FDM products, due to the nature of the process itself: since the specimens are built layer-by-layer, a tensile load will be directed parallel to the layers in a “flat” part, while it will be perpendicular in an “upright” (fig.4.1, taken from [36]).

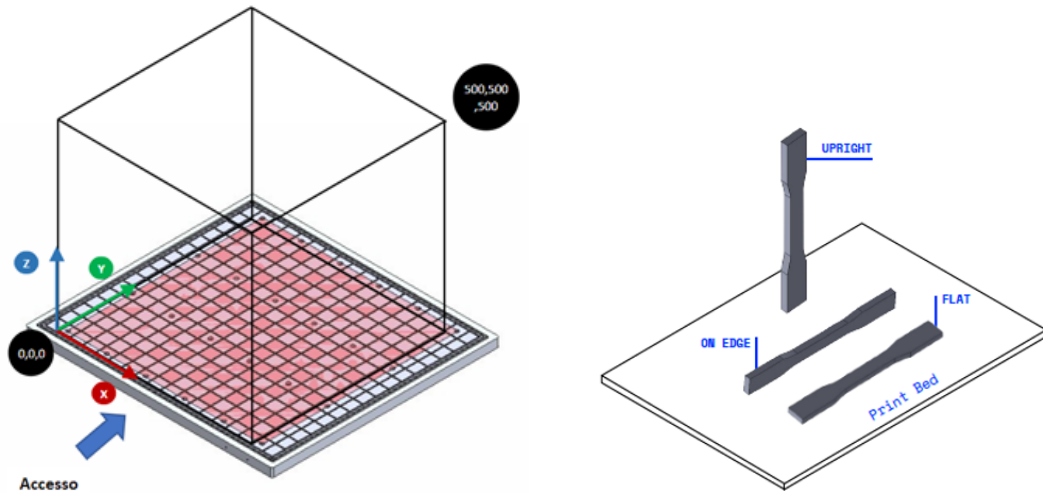


Figure 4.1: a) Axes directions with respect to the building platform, b) Different building orientations of the same part.

- Infill rate: this value indicates the material filling of the part; it can vary from 0% (totally empty), to 100% (completely filled), and the two selected values for the thesis are 100% and 35%. This parameter directly influences the quantity of material that has to be used, and consequently it affects the mechanical performance of the part and the printing time. As it can be seen in fig.4.2 (taken from [44]), the infill rate regards the internal part of the product, while the wall layers (i.e., the layer constituting the contour of the piece) are not affected by its variations; the number of wall layers can however be modified separately.
- Testing temperature: it is known that temperature deeply affect the performance of a material, changing, for instance, its elasticity modulus. Moreover, the applications of *Punch* AM products may regard high temperature situations, so it is surely useful to determine the behaviour of ULTEM™ and Carbon PEEK in not standard conditions. For this purpose, some batches have been tested at environmental temperature (20°C), some others at 120°C, without exceeding the glass transition temperature of the two materials, beyond which they would soften.

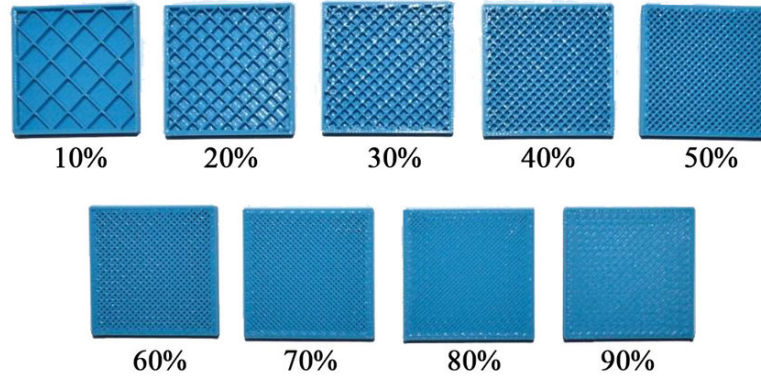


Figure 4.2: Different infill rates for the same part

Having four variables that could assume two different values, it was easy to determine that the number of possible combinations is $2^4 = 16$. This means that, ideally, sixteen different specimens (whose shape depended on the reference Standard choice, cfr. par.4.2) should be printed and tested to completely cover all the cases. A test matrix could be created, containing all the parameters characterizing each version of the artifact (tab.4.1).

	material	orientation	infill rate	test temperature	
1	Carbon PEEK	xy	100%	ambient	1
2				120°C	2
3			35%	ambient	3
4				120°C	4
5		zx	100%	ambient	5
6				120°C	6
7			35%	ambient	7
8				120°C	8
9	ULTEM™	xy	100%	ambient	9
10				120°C	10
11			35%	ambient	11
12				120°C	12
13		zx	100%	ambient	13
14				120°C	14
15			35%	ambient	15
16				120°C	16

Table 4.1: Test matrix

4.2 ASTM D638

ASTM D638-2014[45] was the selected Standard for the tensile tests. This choice mainly depended on two factors:

1. Researching on websites as *Google Scholar* or *Research Gate*, it was the most utilized normative for tensile tests, followed by ISO 527; these two can be considered almost equivalent, however D638 was generally preferred by other authors (e.g., [46][47]).
2. The tests made by *Roboze*, whose results are collected into the official Technical Data Sheets, were done following ASTM D638; using the same standard, the outcomes were surely more comparable. Following this aspect, many influencing parameters in this thesis have been maintained the same as in the TDS, in particular the type of specimen and the speed of testing.[36][31]

It must be highlighted that currently there are a very restricted number of Standards written specifically for Additive Manufacturing; ASTM D638 itself is generically applicable to any kind of plastics, without taking into account the production method.

This Standard prescribes the usage of dog-bone shaped specimens, to whom a tensile load must be applied until their breaking, if possible. As it can be seen in figure 4.3[45], the central part of these pieces has a smaller cross section with respect to the extremities, and it is the area where they should break to consider the test valid. In figure 4.4[45] the reference dimensions are reported: some of the are fixed, some others can be adapted to the specific equipment.

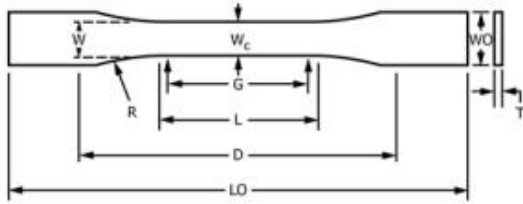


Figure 4.3: Design of the specimen for the tensile test

Dimensions (see drawings)	7 (0.28) or under	
	Type I	Type II
W—Width of narrow section ^{E,F}	13 (0.50)	6 (0.25)
L—Length of narrow section	57 (2.25)	57 (2.25)
WC—Width overall, min ^G	19 (0.75)	19 (0.75)
WC—Width overall, min ^G
LO—Length overall, min ^H	165 (6.5)	183 (7.2)
G—Gage length ^I	50 (2.00)	50 (2.00)
G—Gage length ^I
D—Distance between grips	115 (4.5)	135 (5.3)
R—Radius of fillet	76 (3.00)	76 (3.00)
RO—Outer radius (Type IV)

Figure 4.4: Reference dimensions for the specimen

The most important parameter to be determined is the thickness of the specimen (T in fig.4.4), since it directly influences the minimal cross section of the artifact and, consequently, its resistance. To be sure to collect a proper number of data for

all the specimens, it was necessary to calculate the minimum T which allowed the theoretically weakest piece to bear a load of 2000 N. Starting from the official TDS of ULTEM™ and Carbon PEEK, the lowest foundable σ_{break} was 28.2 MPa (Carbon PEEK, 100% infill, 25°C, zx orientation) and the relative minimum thickness was calculated in the following way:

$$\sigma_{break} = \frac{F_{break}}{A_{minimalcrosssection}} \rightarrow$$

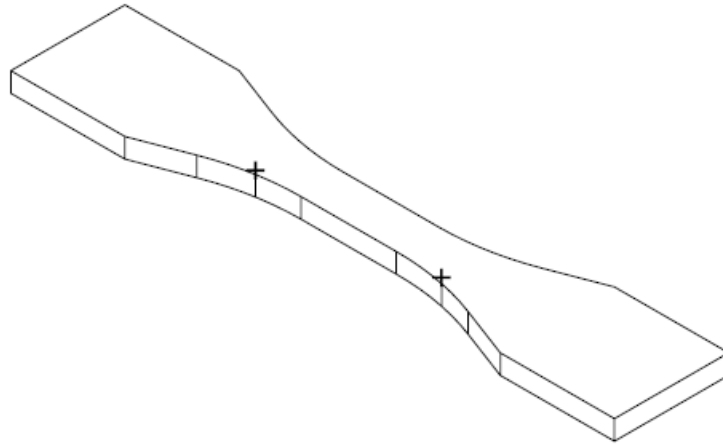
$$\rightarrow A_{minimalcrosssection} = \frac{F_{break}}{\sigma_{break}} = \frac{2000N}{28.2MPa} = 70.9mm^2$$

$$A = W \times T \rightarrow$$

$$\rightarrow T_{min} = \frac{A_{minimalcrosssection}}{W} = \frac{70.9mm^2}{13mm} = 5.45mm \rightarrow T_{spec} = 6mm$$

Furthermore, in order to avoid the slipping of the specimens during the test, the extremities' dimensions of the part were augmented by increasing the overall length LO and the overall width WO ; they were influenced by the size of the grippers of the *Instron*.

The final isometric design and measures of the specimen are reported respectively in figures 4.5, 4.6 and table 4.2.



ISOMETRIC VIEW

Figure 4.5: Design of the ultimate specimen

Dimensions	Value [mm]
LO - length overall	185
L - length of narrow section	57
R - radius of fillet	76
WO - width overall	35
T - thickness	6
W - width of narrow section	13

Table 4.2: Ultimate dimensions of the specimens

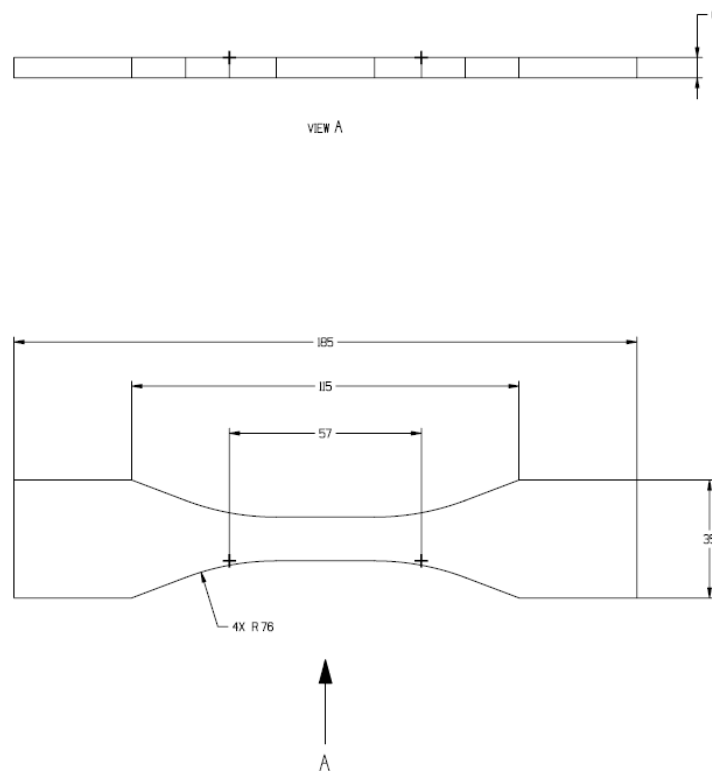


Figure 4.6: Dimensions of the ultimate specimen

The subsequent step was making some test prints to check firstly the effective capability of the machine to properly create the specimens, both horizontally and vertically; due to the higher costs of Carbon PEEK and ULTEM™, in this phase the parts were created in Ultra-PLA, considering also that they were needed only as dimensional prototypes.

The horizontal artifact was good already after the first print, while the vertical one was affected by the over-heating effect: this phenomenon happens when the layers

are so small that they have not enough time to cool down before the following one is created; this causes the lower layers to be partially liquid when the upper ones get deposited, and the result is not as precise as desired (fig.4.7).

The overheating problem could be easily solved by printing more than one vertical specimen during the same job, giving each part more some more seconds to solidify. In particular, five identical items were created, but another issue arised: the layers in the upper sections were not perfectly aligned, meaning that the parts vibrated during the printing operations. The vibrations were due to the fact that the specimens are very slim so they tended to flex when the nozzle was moving. To overcome this problem, two lateral “support-towers” were inserted (fig.4.8).

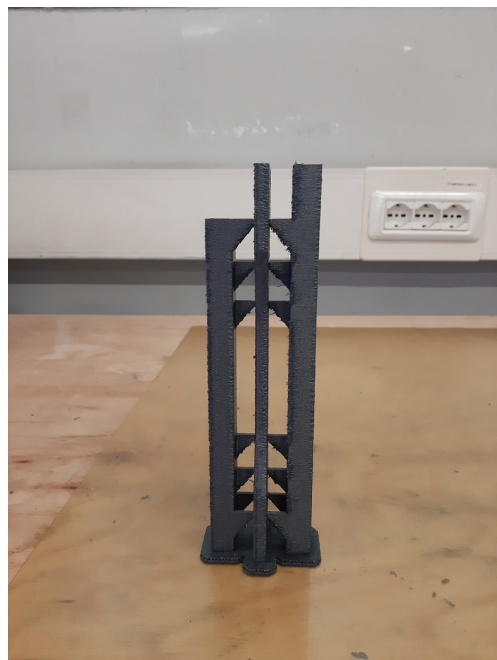


Figure 4.7: Ultra PLA: horizontal (left) and vertical (right) overheated specimen **Figure 4.8:** C-PEEK: vertical specimen with two support towers

After reaching a good result for both the configurations, some preliminary tests in Carbon PEEK and ULTEM™ were also made. Some difficulties in removing the parts from the buildsheet were encountered, resulting in ruining either the pieces or even the buildsheet (fig.4.9). As a solution, the separation distance was increased during the building preparation with *Simplify3D*. This parameter indicates the gap between the extruder and the building platform during the printing of the first layer; by augmenting its value, the filament coming out from the nozzle gets less pressed and the adhesion among the material and the buildsheet is less severe,

facilitating the post-processing operations. After these final adjustments, the definitive specimens were ready to be printed and tested.



Figure 4.9: Carbon PEEK: broken buildsheet and ruined specimens after the artifacts' removal

4.3 Printing and Testing

As prescribed by the Standard, a test is considered valid if at least five identical specimens break in the narrow central section. Considering the relatively high cost of the materials and the quite long printing time, especially for the vertical parts (fig.4.10), the specimens were therefore printed in batches composed of five items. When possible, multiple batches were included in the same printing job (fig.4.11).

Although 16 types of specimens were planned (cfr. chapter 4.1), batches 6, 14, 15, 16 were decided not to be printed; this choice was motivated by the following reasons: firstly, data from previous research and from the technical data sheets showed a significant reduction of the mechanical properties of both the materials in the vertical configuration, especially in terms of σ_{break} ; this means that in reality this orientation will be rarely used, unless it is necessary. Some vertical batches were however tested for completeness and to confirm these trends. Secondly, an unforeseeable increase in electricity costs caused *Punch Torino* to limit the usage of all its equipment, including the *Roboze* printer, temporarily reducing the daily



Figure 4.10: ULTEM: complete vertical batch



Figure 4.11: C-PEEK: four horizontal batches in the printer

available printing time; since vertical batches were quite long to be made, and considering also the hours devoted to the heating of the chamber, they were practically impossible to be created. Fortunately, the majority of the specimens had already been printed before the application of this regulation.

In total, 60 specimens were printed, completely following the procedures regarding pre- and post-processing. The default temperatures and timings (e.g., pre-conditioning of the chamber, drying of the coils, etc.) were respected in order to guarantee an optimal result.

Each artifact was tagged by a letter and a number (e.g., “A1”), to quickly identify its characteristics and its testing temperature. Moreover, also the actual measures of thickness and width in the restricted sections had to be found using a caliper and averaging three different values for both the parameters, in order to calculate the tensile stress σ acting on the parts; all the final W and T are reported in Appendix B, and it can be noticed that all the thicknesses are higher than the nominal T (6 mm), while the widths are generally less than 13 mm for the horizontal specimens and more for vertical ones. Numbering the batches as the specimen’s types in table 4.1, it resulted:

batch	specimens		batch	specimens	
	from	to		from	to
1	A1	A5	8	D6	D10
2	A6	A10	9	E6	E10
3	B1	B5	10	E1	E5
4	B6	B10	11	F1	F5
5	C6	C10	12	F6	F10
7	D1	D5	13	G1	G5

Table 4.3: Labels of the specimens

The tests were made at Politecnico di Torino – DIMEAS department, using an *Instron 8801 machine*. The specimen was locked using two couples of grippers; the upper couple was connected to a mobile crossbar which moved upwards, applying a tensile load to the piece. Above it, a 100 kN load cell was present to measure the applied force F , which divided by the cross-section area $A = W \times T$ gave the tensile stress σ . When possible, the deformation values ϵ were acquired using an extensometer; if not, they were calculated dividing the displacement by the initial gage length: this happened for some ULTEMTM batches, when it was not safe to use the extensometer due to the possibly excessive elongation of the specimens. The longitudinal modulus, or Young's modulus E , could also be evaluated, either directly by the software *Bluehill*, or as the ratio $\frac{\Delta\sigma}{\Delta\epsilon}$, which corresponds to the angular coefficient of the initial part of the stress-strain curve, which can be considered almost linear at low ϵ . To sum up the procedure:

- The software was provided with the measures of the specimen's thickness T and width W , through which it calculated the cross-section area A . Also, the speed of test was chosen to be 5 mm/min.
- The specimen got mounted on the machine and blocked. The closure of the clamps was automatic for the ambient temperature tests, while it was manual for high temperature ones.
- If needed, the extensometer was positioned in the central part of the specimen (fig.4.12a).
- At this point, batches 2, 4, 8, 10, 12 have been heated up to 120°C: this operation happened into a dedicated oven and lasted about 10 minutes for each specimen, to be sure that the whole system reached the desired temperature (fig.4.12b).
- The test began and went on until the rupture of the piece under examination (fig.4.13). The *Instron* acquired data about the displacement of the

upper clamp ($\Delta L[mm]$) and about the tensile load ($F[N]$); the extensometer measured the deformation ($\epsilon[mm/mm]$).

- The machine stopped and each element could be removed.

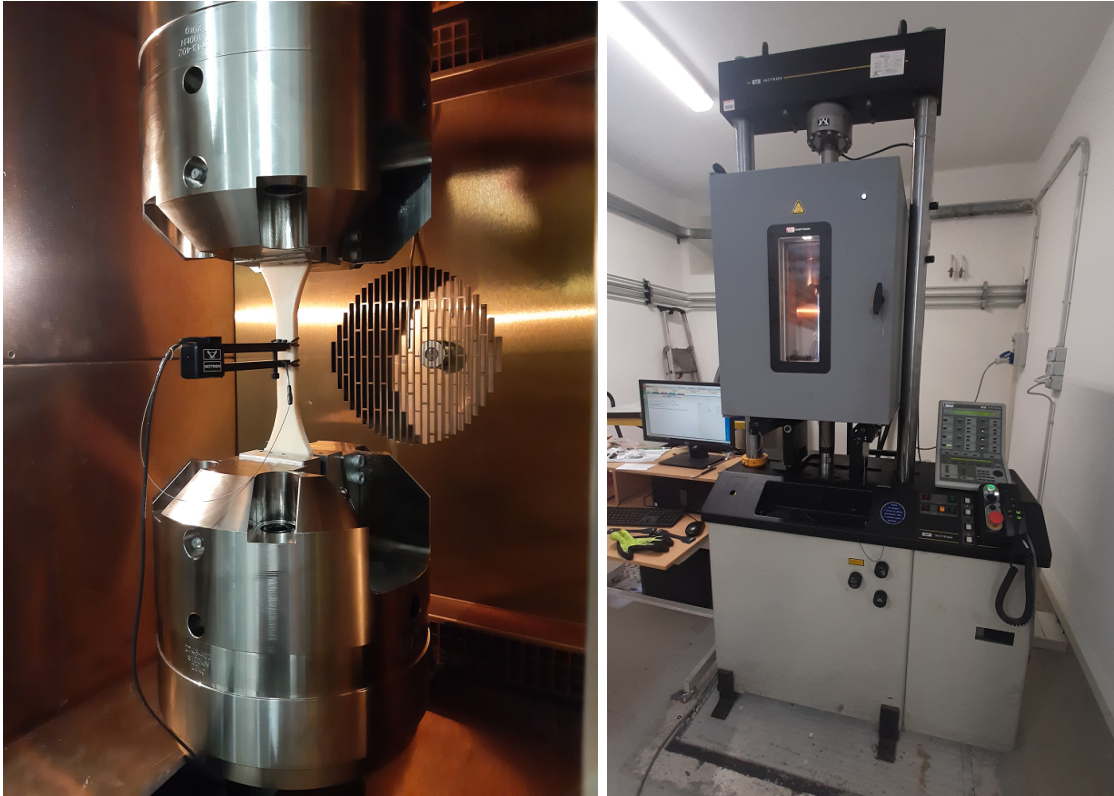


Figure 4.12: a) specimen with extensometer; b) *Instron 8801* set for high temperature tests

An *Excel* file containing all the information and the measures was automatically created by the software, ready to be used for the data analysis. Also, a recap file for each batch was generated, containing all the important values and, for instance, their average, standard deviation and coefficient of variation (COV): the latter was very important to evaluate the dispersion of the obtained data and consequently their reliability. These files allowed the creation of the load-displacement and stress-strain graphs reported in the following sections.

In this case, all the specimens were valid since the fractures happened in the narrow section (fig.4.14). If even only one artifact did not break in the central part, its batch would have been discarded, unless another identical item was tested.



Figure 4.13: Broken specimen at the end of the test



Figure 4.14: Selection of broken specimens

4.4 Results and Comments

4.4.1 Load vs Displacement diagrams

Exploiting the data about the tensile load applied on the part and about the movement of the mobile crossbar of the machine, the load vs displacement diagrams can be drawn. Since their trend is exactly the same of the stress vs strain ones, only two cases will be reported (fig.4.15). It can be seen that batch 1 (Carbon PEEK) is characterized by a more linear trend with respect to batch 9 (ULTEM™); moreover, when the rupture comes, the former specimens instantly break, while the latter ones clearly yield.

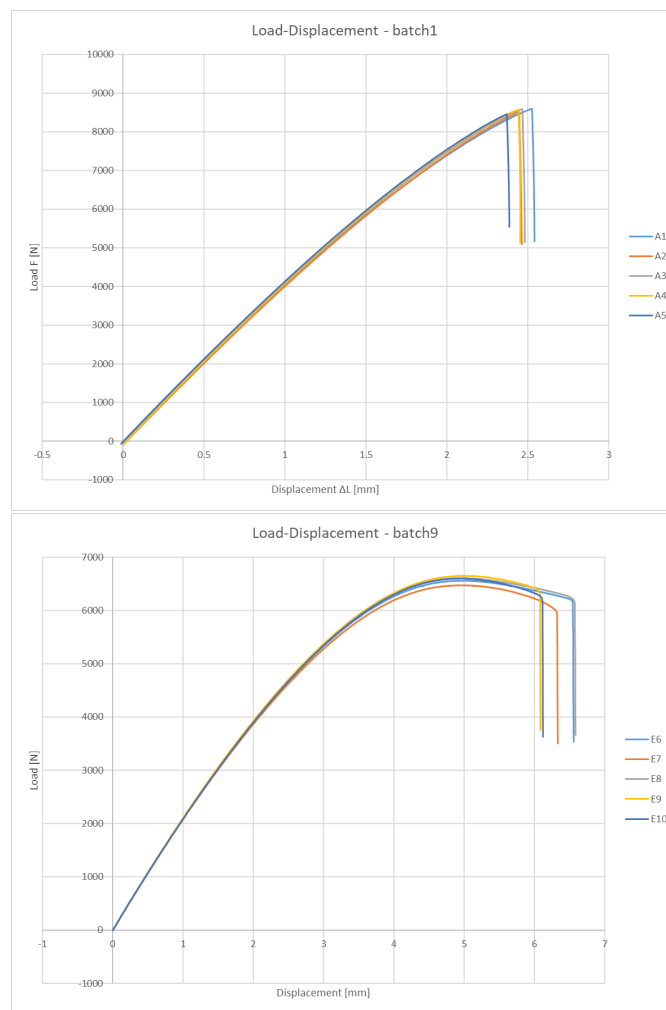
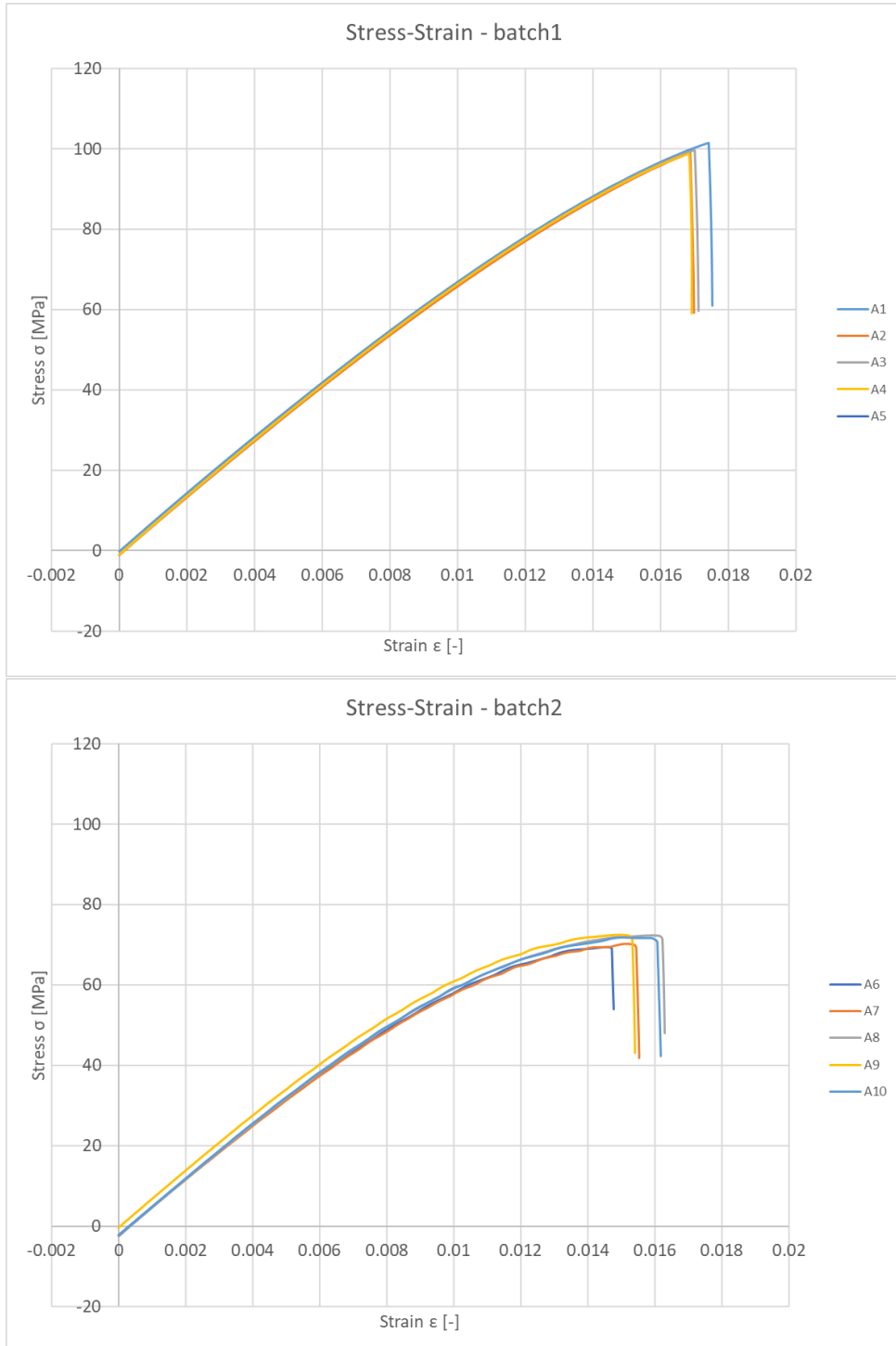
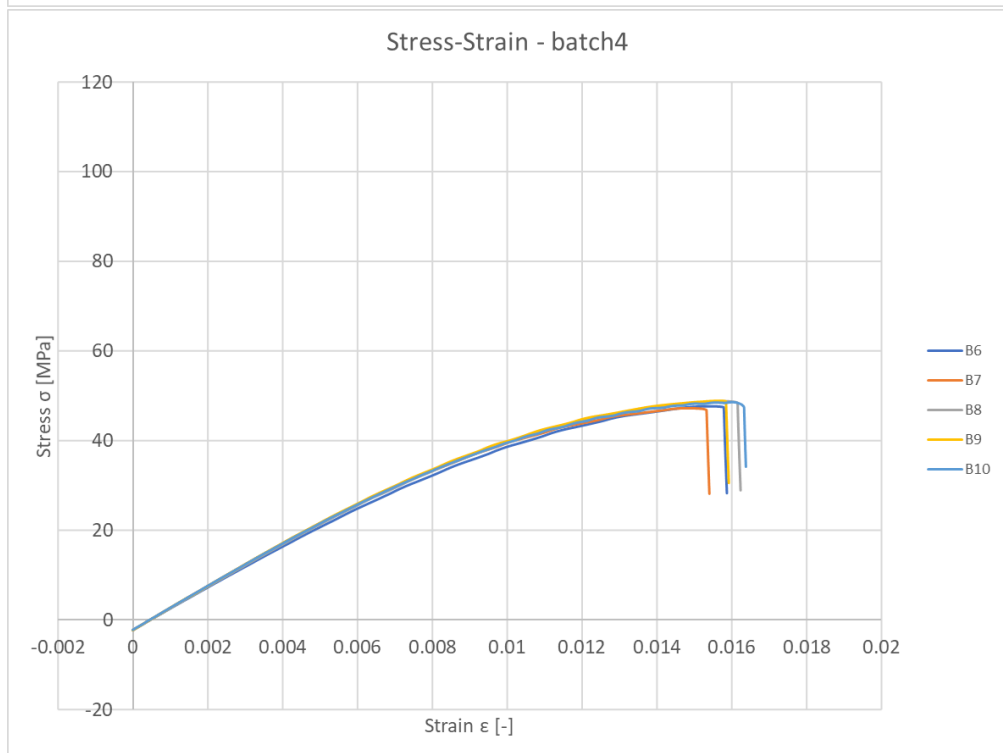
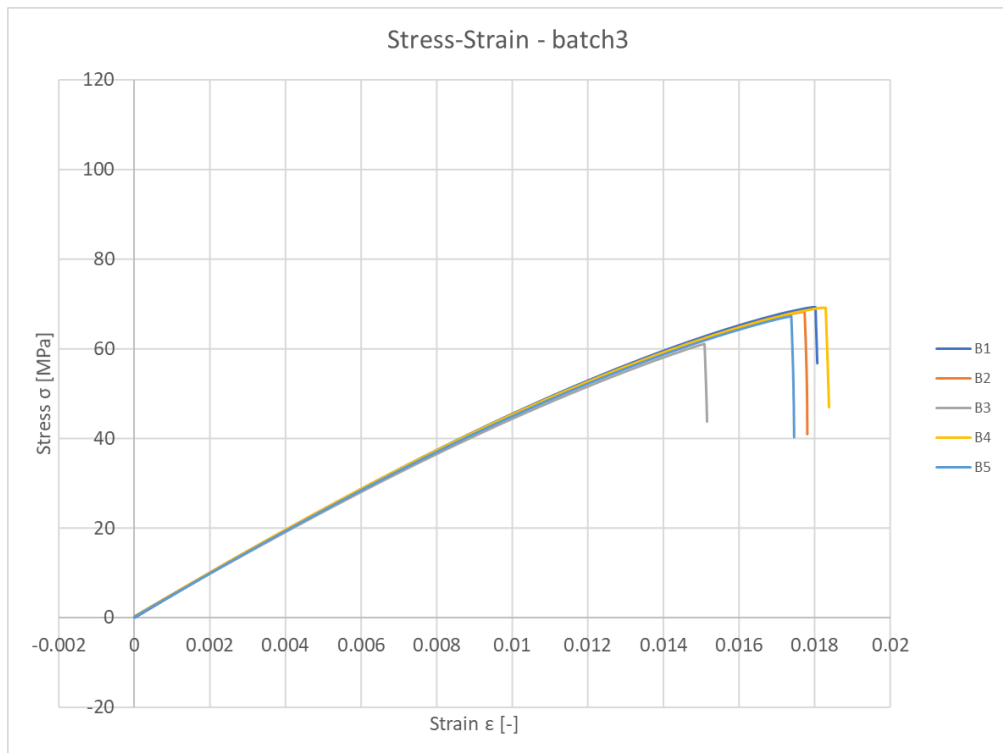
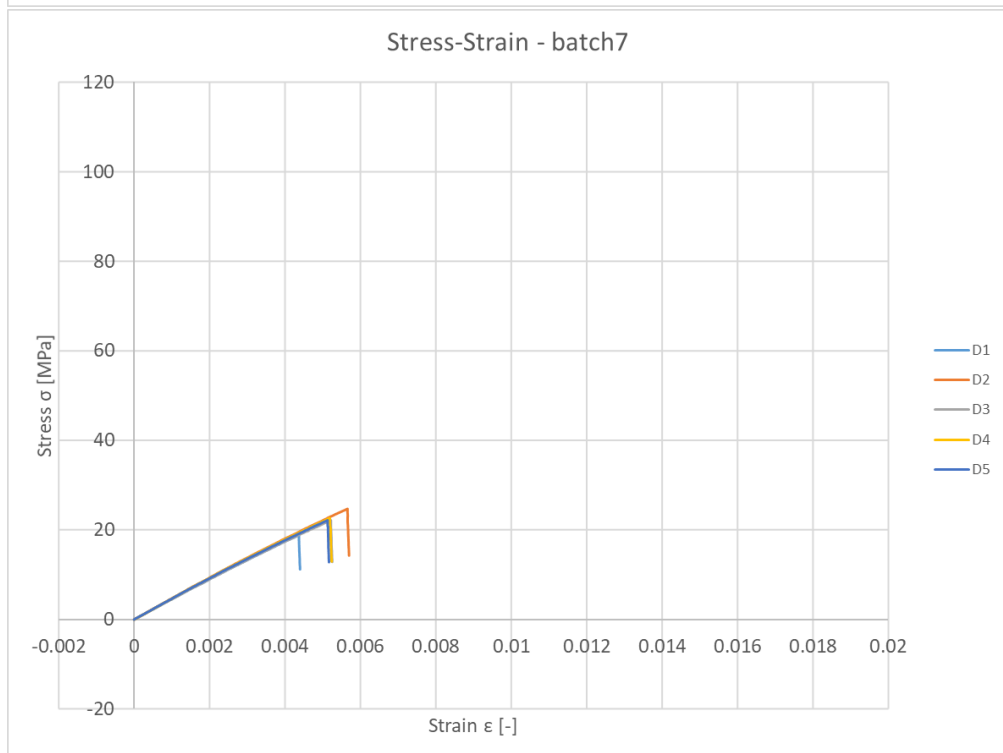
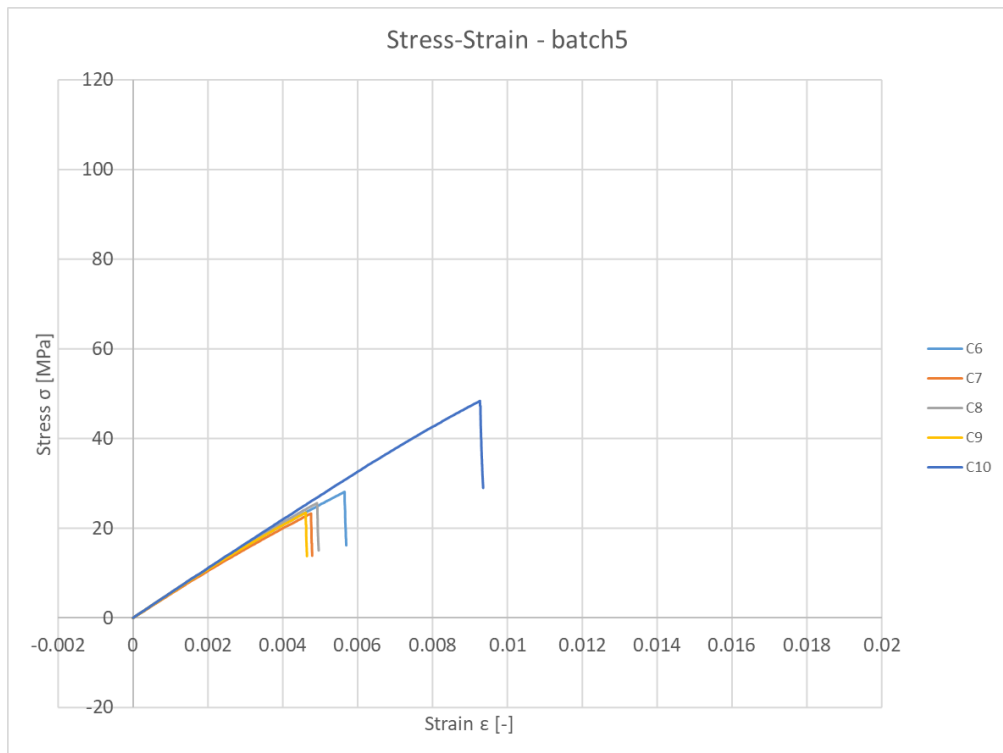


Figure 4.15: Batches 1 and 9 - load vs displacement

4.4.2 Stress vs Strain diagrams - Carbon PEEK







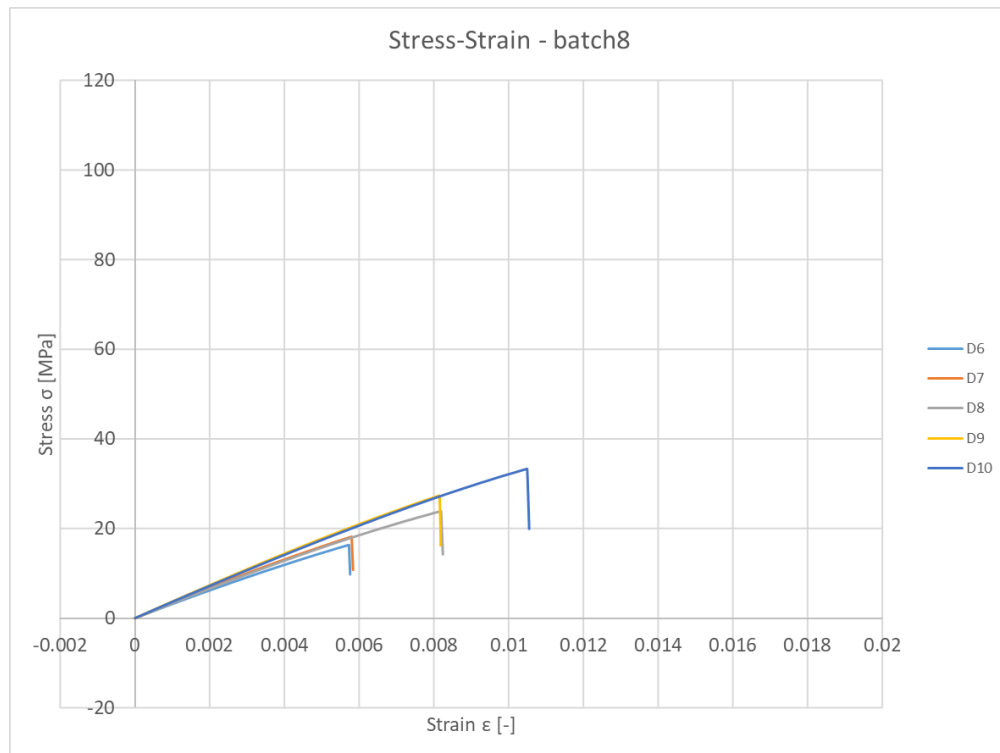
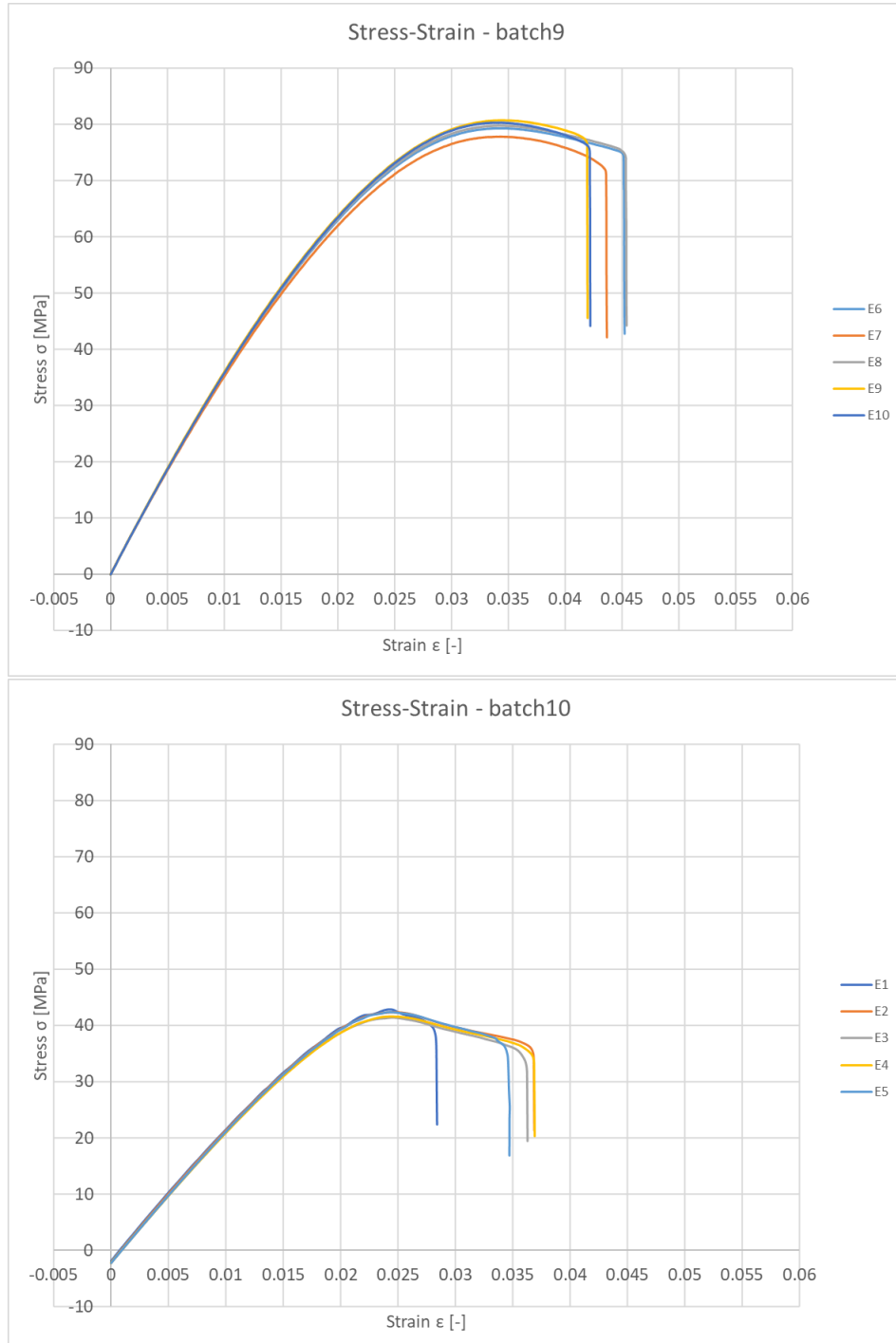


Figure 4.16: Carbon PEEK: stress vs strain diagrams

Looking at the graphs, it is clearly visible that Carbon PEEK does not yield before breaking. All the curves are monotonically crescent, with almost constant slopes, except for batches 2 and 4 where the tensile modulus decreases as it approaches the rupture point. Some particularities can be evidenced:

- Batch 3: specimen B3 failed a little bit before the others.
- Batch 5: specimen C10 strangely bore more load and its slope is higher.
- Batch 8: the results are very scattered. Specimens D6 and D7 broke quite soon, D10 failed later with respect to the others; moreover each artifacts cracked at different stress levels.

4.4.3 Stress vs Strain diagrams - ULTEM™



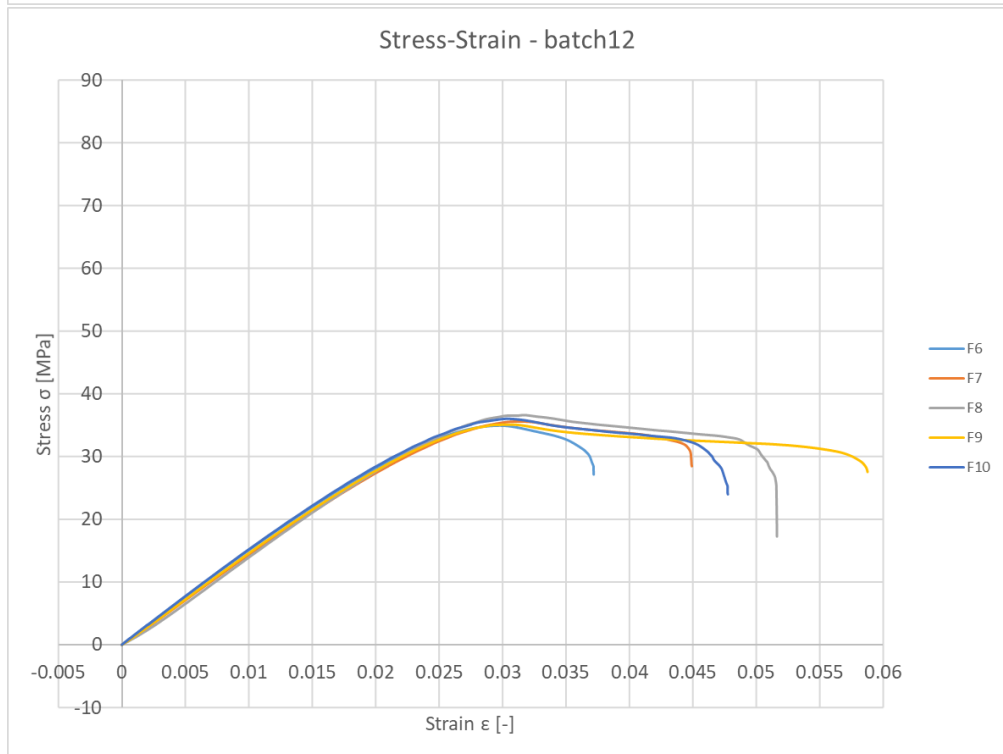
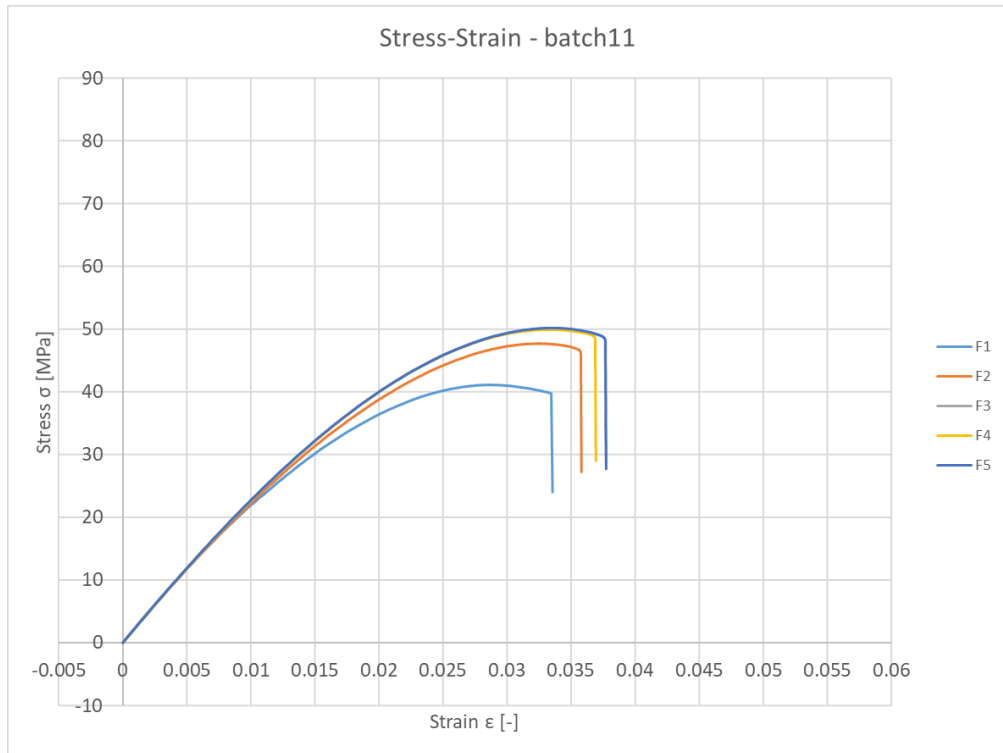




Figure 4.17: ULTEM™: stress vs strain diagrams

ULTEM™ shows a more ductile behaviour with respect to Carbon PEEK; all the batches (except b.13) clearly demonstrate that the material yielded before breaking. Again, some particularities can be highlighted:

- Batch 11: specimen F1 broke a little sooner than the others.
- Batch 12: until the yielding point, all the specimens behaved equally; then, they elongated differently. However, the σ_{break} is quite constant.
- Batch 13: the specimens did not yield, suggesting that the vertical printing orientation may have caused this different trend: the layers were in fact perpendicular to the load.

4.4.4 Results and Analysis

batch	material	print orientation	infill rate	test temperature	σ_{yield} MPa	σ_{break} MPa	E MPa	
1	C-PEEK	horizontal	100%	env	x	99	7256	
2				120°C	x	71	7160	
3			35%	env	x	67	5037	
4				120°C	x	48	4932	
5		vertical	100%	env	x	30	3741	
6				120°C	not printed			
7			35%	env	x	22.5	3023	
8				120°C	x	24	2895	
9	ULTEM™		horizontal	100%	env	80	75	3566
10					120°C	44	35	2256
11		35%		env	48	46	2179	
12				120°C	35	27	1470	
13		vertical	100%	env	x	55	3486	
14				120°C	not printed			
15			35%	env	not printed			
16				120°C	not printed			

Table 4.4: Results of the tensile tests

Some considerations can be made about the obtained results.

Validity of the test As already said, all the specimens broke in the restricted part, so they can be considered valid. However, some numerical results may be less reliable than others, due to higher coefficients of variation: if this value is high, it means that the specimens belonging to the batch behave quite differently from each other, giving more uncertainty about the results. The best example of this situation is batch 8: for completeness, the set will however be considered during the analysis of the data, keeping in mind that “strange” results may be due to its particular behavior.

General trends As expected, batches 1 and 9 are characterized by the highest σ_{break} and E respectively for the Carbon PEEK and the ULTEM™ specimens. In fact, their characteristics (horizontal orientation, 100% infill rate and testing at ambient temperature) suggested they would have been the best sets. Figures 4.18 and 4.19 respectively show the trend of σ_{break} and E for the two materials:

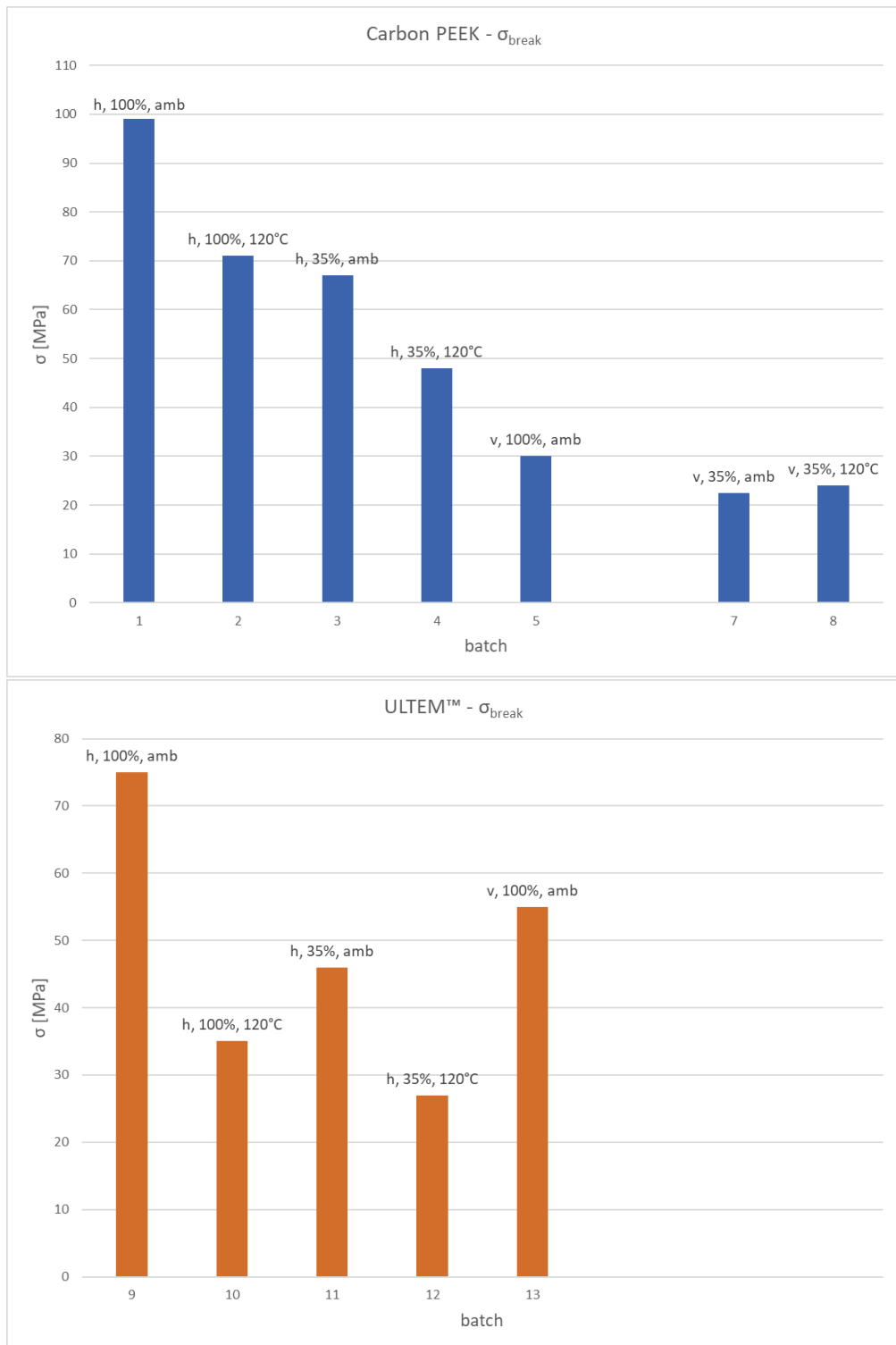


Figure 4.18: Values of σ_{break}

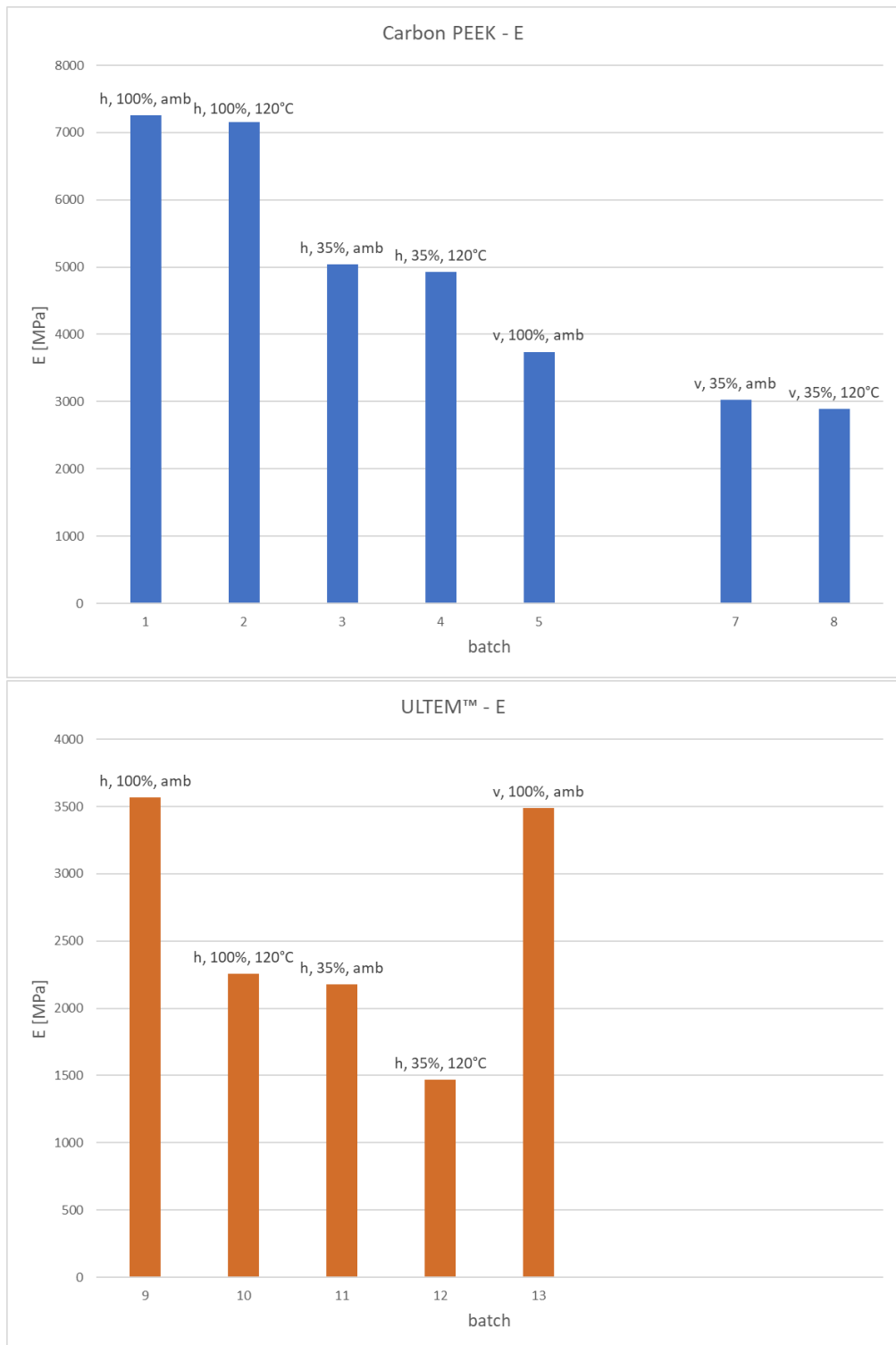


Figure 4.19: Values of E

Numerically speaking, Carbon PEEK is stronger than ULTEM™, as expected. Analyzing the trend it can be easily seen that the printing orientation deeply affect the performance of Carbon PEEK (batches from 5 to 8 are significantly weaker), while ULTEM™ is less influenced, since the difference between sets 9 and 13 is not as wide as, for instance, 1 and 5. Moreover, the resistance of batch 2 is higher than the ones of batches 3 and 5, suggesting that the higher temperature affected Carbon PEEK less with respect to a lower infill rate or a different printing orientation, but it must be taken into account that considering a different temperature and/or a different infill rate the situation may change; the same considerations can be made for ULTEM™, where the higher temperature caused the more evident drop of performances. These graphs highlight some interesting facts: as regards Carbon PEEK, its Young's modulus is almost completely independent from the testing temperature since it doesn't change between batches 1-2, 3-4, and 7-8; differently, 35% infilled specimens and vertical ones are characterized by a lower E . Considering ULTEM™, sets 9 and 13 have quite the same tensile modulus, suggesting that the printing orientation does not affect it (unfortunately this trend cannot be confirmed since the last batches could not be printed); on the other hand, a temperature increase makes E decrease (9-10, 11-12), and also an infill rate reduction has the same effect (9-11, 10-12).

As already said, all the previous statements refer to particular conditions. To confirm the trends, some intermediate cases should be also evaluated (e.g., 50% infill rate, 80°C tests...), trying to derive, if possible, a mathematical law approximating them.

Now each parameter will be treated separately, to check which of them has effectively had more impact. The unit of measure is [MPa] for all the factors, while the resulting ratios are obviously non-dimensional.

Effect of the orientation

$$\begin{aligned} & \sigma_{break} \text{ CarbonPEEK} \\ \frac{batch5}{batch1} = \frac{30}{99} = \mathbf{0.303}; & \frac{batch7}{batch3} = \frac{22.5}{67} = \mathbf{0.335}; \frac{batch8}{batch4} = \frac{24}{48} = \mathbf{0.500} \\ & \sigma_{break} \text{ ULTEM}^{TM} \\ \frac{batch13}{batch9} = \frac{55}{75} = \mathbf{0.733} \\ & E \text{ CarbonPEEK} \\ \frac{batch5}{batch1} = \frac{3741}{7256} = \mathbf{0.516}; & \frac{batch7}{batch3} = \frac{3023}{5037} = \mathbf{0.600}; \frac{batch8}{batch4} = \frac{2895}{4932} = \mathbf{0.587} \\ & E \text{ ULTEM}^{TM} \end{aligned}$$

$$\frac{batch13}{batch9} = \frac{3486}{3566} = \mathbf{0.978}$$

Calculating the ratios among the rupture stress of corresponding vertical and horizontal batches, it appears that vertical Carbon PEEK specimens are even 70% weaker than horizontal ones, while ULTEM™ is less affected. As regards the Young's modulus, ULTEM™ is almost not affected, while Carbon PEEK becomes less rigid, with a decrement of 40-50% from the original value.

Effect of the infill rate

$$\begin{aligned} & \sigma_{break} \text{ CarbonPEEK} \\ \frac{batch3}{batch1} &= \frac{67}{99} = \mathbf{0.677}; \frac{batch4}{batch2} = \frac{48}{71} = \mathbf{0.676}; \frac{batch7}{batch5} = \frac{22.5}{30} = \mathbf{0.750} \end{aligned}$$

$$\begin{aligned} & \sigma_{break} \text{ ULTEM}^{TM} \\ \frac{batch11}{batch9} &= \frac{46}{75} = \mathbf{0.613}; \frac{batch12}{batch10} = \frac{27}{35} = \mathbf{0.771} \end{aligned}$$

$$\begin{aligned} & E \text{ CarbonPEEK} \\ \frac{batch3}{batch1} &= \frac{5037}{7256} = \mathbf{0.694}; \frac{batch4}{batch2} = \frac{4932}{7160} = \mathbf{0.689}; \frac{batch7}{batch5} = \frac{3023}{3741} = \mathbf{0.808} \end{aligned}$$

$$\begin{aligned} & E \text{ ULTEM}^{TM} \\ \frac{batch11}{batch9} &= \frac{2179}{3566} = \mathbf{0.611}; \frac{batch12}{batch10} = \frac{1470}{2256} = \mathbf{0.652} \end{aligned}$$

Except for some ratios, the 35% infilled specimens experience an average reduction of 30-40% for both σ_{break} and E with respect to the corresponding completely full ones. In the case of Carbon PEEK, low-infilled horizontal specimens are stronger than full vertical ones (cfr. Batches 3 and 5). As regards ULTEM™, in this case reduction of the tensile modulus is evident, differently from the previous case.

Effect of the test temperature

$$\begin{aligned} & \sigma_{break} \text{ CarbonPEEK} \\ \frac{batch2}{batch1} &= \frac{71}{99} = \mathbf{0.717}; \frac{batch4}{batch3} = \frac{48}{67} = \mathbf{0.716}; \frac{batch8}{batch7} = \frac{24}{22.5} = \mathbf{1.07} \end{aligned}$$

$$\begin{aligned} & \sigma_{break} \text{ ULTEM}^{TM} \\ \frac{batch10}{batch9} &= \frac{35}{75} = \mathbf{0.467}; \frac{batch12}{batch11} = \frac{27}{46} = \mathbf{0.587} \end{aligned}$$

$$\begin{aligned} & E \text{ CarbonPEEK} \\ \frac{batch2}{batch1} &= \frac{7160}{7256} = \mathbf{0.987}; \frac{batch4}{batch3} = \frac{4932}{5037} = \mathbf{0.979}; \frac{batch8}{batch7} = \frac{2895}{3023} = \mathbf{0.958} \end{aligned}$$

E ULTEMTM

$$\frac{batch10}{batch9} = \frac{2256}{3566} = \mathbf{0.632}; \frac{batch12}{batch11} = \frac{1470}{2179} = \mathbf{0.675}$$

Finally, the effect of test temperature is more evident for ULTEMTM artifacts, which experience a not indifferent reduction of both the researched parameters. Regarding Carbon PEEK, its σ_{break} is affected by reduction of 39% (it must be noticed that one ratio is major than 1, which is quite strange, but it may be due to the not completely reliable results regarding batch 8); the Young's modulus, on the other hand, is almost unaffected by the temperature.

Yielding For all the ULTEMTM batches, except batch 13, a yielding stress σ_{yield} can be identified, as reported in the previous table.

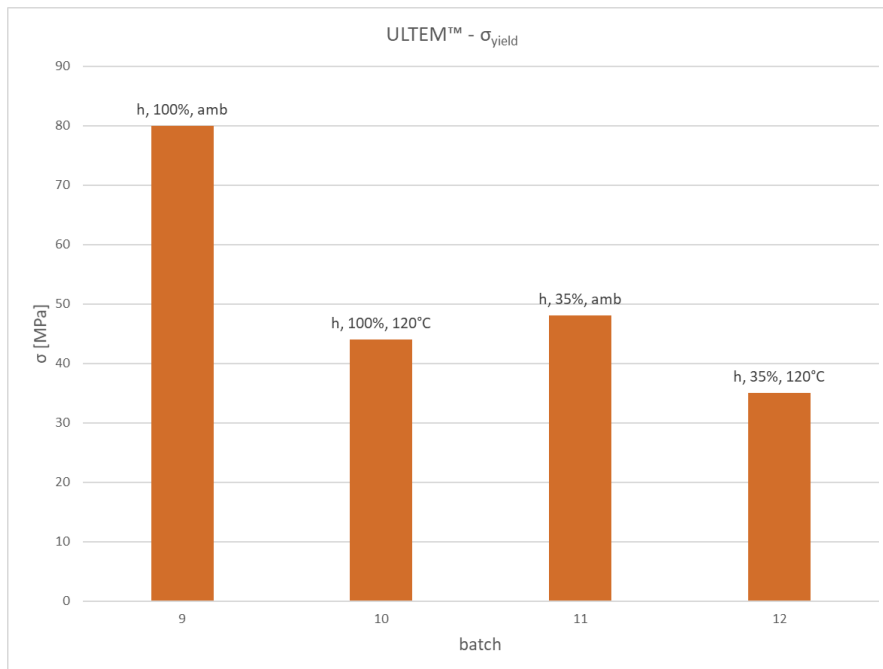


Figure 4.20: Values of σ_{yield}

As before, the ratios between the different stresses can be calculated to evaluate the reduction of the performances. In this case, all the sets are horizontally oriented.

Effect of the infill rate

$$\sigma : \frac{batch11}{batch9} = \frac{48}{80} = \mathbf{0.600}; \frac{batch12}{batch10} = \frac{35}{44} = \mathbf{0.795}$$

Effect of the test temperature

$$\sigma : \frac{batch10}{batch9} = \frac{44}{80} = \mathbf{0.550}; \frac{batch12}{batch11} = \frac{35}{48} = \mathbf{0.729}$$

Considering the chosen parameters, the testing at 120°C makes the yielding stress reduce more than reducing the infill to 35% (0.550 against 0.600). It does not make sense repeating the calculations for E since it is the same as in the previous cases.

Chapter 5

Conclusions

The topic of this Thesis was the implementation of a new industrial process at *Punch Torino S.p.A*, based on the Fused Deposition Modelling technique. In particular, the performance of the newly acquired *Roboze Argo 500* printer was investigated by means of capability assessments, following the ISO/ASTM 52902 Standard. Analysing the results, it can be understood with which material a particular feature is replicated in the best way. The sets of major interest were the ones printed in ULTEM™ and Carbon PEEK, the analysis of the results is summed up in table 5.1:

Artifact	Which material is better?
Linear artifact	Not clear
Circular artifacts	Not clear
Resolution Pins artifacts	ULTEM™
Resolution Holes artifacts	Carbon PEEK
Resolution Ribs artifacts	ULTEM™
Resolution Slots artifacts	ULTEM™
Resolution Slotted Angles artifacts	ULTEM™
Surface Texture artifact	Carbon PEEK

Table 5.1: Capability assessments comparison: Carbon PEEK and ULTEM™

Identical capability assessments were conducted for the others 3D printers owned by *Punch*, or with the same printer but using different materials. The complete results are collected in Appendix B. Moreover, a further test using different artifacts was necessary to certify the correct functioning of the *Argo 500*, and all the specimens turned out to be conform.

Then, the mechanical properties of ULTEM™ and Carbon PEEK were studied performing a series of tensile tests (ASTM D638) at Politecnico di Torino. The

main goal was understanding if and how some changes in the printing parameters of the specimens would affect the breaking and the yielding stresses (σ_{break} , σ_{yield}) and the Young's Modulus (E). As expected, a reduction of all these values happened in case of:

- Vertical printing orientation rather than horizontal,
- Reduction of the infill rate (35% versus 100%),
- Increment of the testing temperature (120°C versus ambient).

A total of 60 specimens were tested, divided into 12 batches composed of 5 identical artifacts; each batch was characterized by a certain combination of the three previously listed parameters: orientation, infill rate and testing temperature. No specimens were discarded since all the fractures occurred in their central part; however, results about batch 8 may be as not reliable as the others due to a very high dispersion of the values.

Analysing the results collected in table 4.4, it can be highlighted that Carbon PEEK seems not to be affected by the temperature increase, while the change in the printing orientation did not alter the mechanical performance of ULTEM™.

The obtained results match the initial expectations suggested by the values contained in the Technical Data Sheets of the materials; moreover, they can be used as a starting point or as an integration for deeper resources about Additive Manufacturing materials. Further investigations may be done by considering some other values of the already selected parameters, for instance a 50% infill rate or testing at 100°C, and check if a mathematical rule describing the alteration of the mechanical properties can be found by interpolating the results. Alternatively, some other printing parameters may be considered, even if this would exponentially increase the number of possible combinations. Eventually, analysis regarding flexural, compressive and fatigue behaviours could be interesting to fully describe the performance of the materials.

Appendix A

Capability Assessment

In the following the results of the capability assessments that have not been treated in chapter 3 are reported. The acronyms in the tables stand for:

- X7: *Markforged X7*, Onyx
- Pro: *Markforged OnyxPro*, Onyx
- S5: *Ultimaker S5*, PLA
- PLA: *Roboze Argo 500*, PLA
- CPA: *Roboze Argo 500*, Carbon-PA

Linear artifact					
Nominal	X7	Pro	S5	PLA	CPA
2.5	2.64	2.79	2.62	2.78	2.61
5	5.16	5.29	5.06	5.26	5.71
5	5.25	5.29	5.06	5.26	5.58
5	5.16	5.19	5.11	5.25	5.77
2.5	2.63	2.69	2.63	2.77	2.61
5	4.88	4.81	4.84	4.79	4.85
7.5	7.31	7.32	7.44	7.22	6.8
10	9.87	9.79	9.93	9.74	9.49
12.5	12.45	12.38	12.35	12.29	11.76

Table A.1: Linear artifact

Circular artifacts					
Nominal	X7	Pro	S5	PLA	CPA
10	9.91	9,88	9.62	9.82	9.96
14	13.94	13.92	13.86	13.35	fail
16	14.97	15,07	14.81	15.29	fail
30	29.99	29.79	29.79	29.76	29.75
47	47.02	46.99	46.84	46.92	46.56
50	50.01	50.10	49.81	49.95	49.75
5	4.91	4.93	4.56	4.87	4.87
7	6.91	6.88	6.61	6.58	fail
8	8.02	8.04	7.79	8.20	fail
15	14.96	14.92	14.76	14.85	14.91
23.5	23.50	23.49	23.38	23.55	23.27
25	25.04	25.09	24.92	25.04	24.71

Table A.2: Circular artifacts

Resolution Pins artifact					
Nominal	X7	Pro	S5	PLA	CPA
4	4.10	4.06	4.03	3.96	3.96
3	3.18	3.11	3.10	3.00	3.16
2	2.25	2.22	2.07	fail	2.15
1	1.29	1.23	1.45	fail	fail

Table A.3: Resolution Pins artifact

Resolution Holes artifact			
Nominal	X7	Pro	S5
4	3.89750	3.92755	3.66250
3	2.87745	2.92985	2.67225
2	1.80585	1.86495	1.61935

Table A.4: Resolution Holes artifact

Resolution Ribs artifacts					
Nominal	X7	Pro	S5	PLA	CPA
6	6.12	6.08	6.07	6.05	6.04
5	5.15	5.10	5.04	5.07	5.02
4	4.19	4.13	4.05	4.06	3.98
3	3.18	3.11	3.04	3.02	3.05
2	2.13	2.05	2.05	2.04	2.03
1	1.16	1.12	1.04	1.15	1.36
1	1.15	1.17	1.05	1.08	1.32
0.8	0.99	0.95	0.90	0.96	1.31
0.6	0.78	0.73	0.71	0.84	fail
0.4	0.66	0.68	fail	fail	fail

Table A.5: Resolution Ribs artifacts

Resolution Slots artifacts					
Nominal	X7	Pro	S5	PLA	CPA
6	5.98	5.76	5.91	5.93	6.09
5	4.97	4.85	4.89	4.92	5.00
4	3.96	3.82	3.89	3.93	4.04
3	3.00	2.77	2.90	2.96	3.00
2	1.99	1.80	1.92	1.96	2.03
1	0,95	0.95	0,95	0.90	1.00
1	0.95	0.95	0.95	1.00	1.00
0.8	0.75	0.75	0.75	0.80	0.80
0.6	0.50	0.60	0.55	0.60	0.50
0.4	fail	fail	0.35	0.40	0.40
0.2	fail	fail	fail	fail	0.20

Table A.6: Resolution Slots artifacts

Resolution Slotted Angles artifacts					
Nominal	X7	Pro	S5	PLA	CPA
6	5.80	5.93	5.92	5.94	5.74
5	4.84	4.91	4.94	4.96	4.86
4	3.82	3.93	3.92	3.96	3.90
3	2.83	2.94	2.92	2.95	2.88
2	1.83	1.94	1.87	1.95	1.89
1	0.95	1.00	0.95	0.90	0.90
1	0.95	0.95	0.95	1.00	1.00
0.8	0.75	0.70	0.75	0.80	0.80
0.6	0.50	0.50	0.55	0.60	0.60
0.4	fail	fail	0.35	0.30	0.30

Table A.7: Resolution Slotted Angles artifacts

Surface Texture artifact			
	X7	Pro	S5
0°	5.571	6.995	9.938
15°	20.373	18.807	9.893
30°	18.898	20.013	10.799
45°	13.798	13.917	20.083
60°	11.507	11.110	21.450
75°	9.900	18.807	17.266
90°	9.875	9.706	4.634

Table A.8: Surface Texture artifact

Appendix B

Measures of the specimens

specimen	W	T	spec	W	T	spec	W	T
A1	13.02	6.51	C6	12.47	6.55	E1	13.02	6.51
A2	13.02	6.61	C7	13.45	6.38	E2	13.02	6.61
A3	13.02	6.62	C8	13.42	6.42	E3	13.02	6.62
A4	13.07	6.64	C9	13.36	6.50	E4	13.07	6.64
A5	12.99	6.63	C10	13.45	6.48	E5	12.99	6.63
A6	13.01	6.62	D1	13.31	6.49	E6	13.01	6.62
A7	13.03	6.64	D2	13.25	6.37	E7	13.03	6.64
A8	12.93	6.60	D3	13.30	6.45	E8	12.93	6.60
A9	12.99	6.56	D4	13.26	6.42	E9	12.99	6.56
A10	13.00	6.59	D5	13.30	6.46	E10	13.00	6.59
B1	12.89	6.58	D6	13.22	6.31	F1	12.89	6.58
B2	12.96	6.63	D7	13.16	6.21	F2	12.96	6.63
B3	12.91	6.65	D8	13.21	6.35	F3	12.91	6.65
B4	12.97	6.63	D9	13.20	6.29	F4	12.97	6.63
B5	12.94	6.66	D10	13.28	6.38	F5	12.94	6.66
B6	12.99	6.63	G1	13.24	6.39	F6	12.99	6.63
B7	12.96	6.63	G2	13.36	6.35	F7	12.96	6.63
B8	12.92	6.63	G3	13.26	6.32	F8	12.92	6.63
B9	12.89	6.62	G4	13.30	6.34	F9	12.89	6.62
B10	12.96	6.63	G5	13.32	6.40	F10	12.96	6.63

Table B.1: Measures of the specimens for the tensile tests

Bibliography

- [1] Jürgen Gausemeier et al. *Additive Manufacturing*. June 2017. ISBN: 978-3-8047-3677-1 (cit. on p. 1).
- [2] L. Iuliano. *Slides of the course Tecniche di Fabbricazione Additiva*. Politecnico di Torino - slides. 2021 (cit. on pp. 1, 5, 9).
- [3] Xingting Han, Dong Yang, Chuncheng Yang, Sebastian Spintzyk, Lutz Scheideler, Ping li, Jürgen Geis-Gerstorfer, and Frank Rupp. «Carbon Fiber Reinforced PEEK Composites Based on 3D-Printing Technology for Orthopedic and Dental Applications». In: *Journal of Clinical Medicine* 8 (Feb. 2019). DOI: 10.3390/jcm8020240 (cit. on pp. 2, 16).
- [4] Camacho A.M. Rodríguez-Panes A. Claver J. «The Influence of Manufacturing Parameters on the Mechanical Behaviour of PLA and ABS Pieces Manufactured by FDM: A Comparative Analysis». In: *Materials* 21 (Aug. 2018), pp. 22–37. DOI: 10.3390/ma11081333 (cit. on pp. 2, 7).
- [5] Ümit Çevik and Menderes Kam. «A Review Study on Mechanical Properties of Obtained Products by FDM Method and Metal/Polymer Composite Filament Production». In: *Journal of Nanomaterials* 2020 (Nov. 2020). DOI: 10.1155/2020/6187149 (cit. on pp. 2, 5).
- [6] Syed A.M. Tofail et al. «Additive manufacturing: scientific and technological challenges, market uptake and opportunities». In: *Materials Today* 21 (1 2018), pp. 22–37. URL: <https://doi.org/10.1016/j.mattod.2017.07.001> (cit. on p. 2).
- [7] Ugur M. Dilberoglu, Bahar Gharehpapagh, Ulas Yaman, and Melik Dolen. «The Role of Additive Manufacturing in the Era of Industry 4.0». In: *Procedia Manufacturing* 11 (2017). 27th International Conference on Flexible Automation and Intelligent Manufacturing, FAIM2017, 27-30 June 2017, Modena, Italy, pp. 545–554. ISSN: 2351-9789. DOI: <https://doi.org/10.1016/j.promfg.2017.07.148>. URL: <https://www.sciencedirect.com/science/article/pii/S2351978917303529> (cit. on p. 2).

- [8] Shu Tay, Lee Te Chuan, A. Aziati, and Ahmad Nur Aizat Ahmad. «An Overview of Industry 4.0: Definition, Components, and Government Initiatives». In: *Journal of Advanced Research in Dynamical and Control Systems* 10 (Dec. 2018), p. 14 (cit. on p. 2).
- [9] K Reddy and Solomon Dufera. «Additive Manufacturing technologies». In: (July 2019) (cit. on p. 2).
- [10] Xinchang Zhang and Frank Liou. «Chapter 1 - Introduction to additive manufacturing». In: *Additive Manufacturing*. Ed. by Juan Pou, Antonio Riveiro, and J. Paulo Davim. Handbooks in Advanced Manufacturing. Elsevier, 2021, pp. 1–31. ISBN: 978-0-12-818411-0. DOI: <https://doi.org/10.1016/B978-0-12-818411-0.00009-4>. URL: <https://www.sciencedirect.com/science/article/pii/B9780128184110000094> (cit. on pp. 3, 4).
- [11] Marco Casini. «Chapter 8 - Advanced building construction methods». In: *Construction 4.0*. Ed. by Marco Casini. Woodhead Publishing Series in Civil and Structural Engineering. Woodhead Publishing, 2022, pp. 405–470. ISBN: 978-0-12-821797-9. DOI: <https://doi.org/10.1016/B978-0-12-821797-9.00006-4>. URL: <https://www.sciencedirect.com/science/article/pii/B9780128217979000064> (cit. on pp. 3, 4).
- [12] S.L. Sing, C.F. Tey, J.H.K. Tan, S. Huang, and Wai Yee Yeong. «2 - 3D printing of metals in rapid prototyping of biomaterials: Techniques in additive manufacturing». In: *Rapid Prototyping of Biomaterials (Second Edition)*. Ed. by Roger Narayan. Second Edition. Woodhead Publishing Series in Biomaterials. Woodhead Publishing, 2020, pp. 17–40. ISBN: 978-0-08-102663-2. DOI: <https://doi.org/10.1016/B978-0-08-102663-2.00002-2>. URL: <https://www.sciencedirect.com/science/article/pii/B9780081026632000022> (cit. on p. 3).
- [13] Ester M. Palmero and Alberto Bollero. «3D and 4D Printing of Functional and Smart Composite Materials». In: *Encyclopedia of Materials: Composites*. Ed. by Dermot Brabazon. Oxford: Elsevier, 2021, pp. 402–419. ISBN: 978-0-12-819731-8. DOI: <https://doi.org/10.1016/B978-0-12-819724-0.00008-2>. URL: <https://www.sciencedirect.com/science/article/pii/B9780128197240000082> (cit. on p. 3).
- [14] Christopher J. Hansen, Amy M. Peterson, and Jay H. Park. «Chapter 23 - 3D printing». In: *Handbook of Thermoset Plastics (Fourth Edition)*. Ed. by Hanna Dodiuk. Fourth Edition. Plastics Design Library. Boston: William Andrew Publishing, 2022, pp. 1021–1043. ISBN: 978-0-12-821632-3. DOI: <https://doi.org/10.1016/B978-0-12-821632-3.00017-8>. URL: <https://www.sciencedirect.com/science/article/pii/B9780128216323000178> (cit. on p. 3).

- [15] Yi Zhang, William Jarosinski, Yeon-Gil Jung, and Jing Zhang. «2 - Additive manufacturing processes and equipment». In: *Additive Manufacturing*. Ed. by Jing Zhang and Yeon-Gil Jung. Butterworth-Heinemann, 2018, pp. 39–51. ISBN: 978-0-12-812155-9. DOI: <https://doi.org/10.1016/B978-0-12-812155-9.00002-5>. URL: <https://www.sciencedirect.com/science/article/pii/B9780128121559000025> (cit. on p. 4).
- [16] Orhan Gülcan, Kadir Günaydın, and Aykut Tamer. «The State of the Art of Material Jetting—A Critical Review». In: *Polymers* 13.16 (2021). ISSN: 2073-4360. DOI: 10.3390/polym13162829. URL: <https://www.mdpi.com/2073-4360/13/16/2829> (cit. on p. 4).
- [17] AMFG. *A comprehensive guide to Material Jetting 3D Printing*. June 2018. URL: <https://amfg.ai/2018/06/29/material-jetting-3d-printing-guide/> (cit. on p. 4).
- [18] Vivianne Bruère, A. Lion, Jens Holtmannspoetter, and M. Johlitz. «Under-extrusion challenges for elastic filaments: the influence of moisture on additive manufacturing». In: *Progress in Additive Manufacturing* 7 (June 2022), pp. 1–8. DOI: 10.1007/s40964-022-00300-y (cit. on p. 5).
- [19] Fredrick Mwema and Esther Akinlabi. «Basics of Fused Deposition Modelling (FDM)». In: May 2020, pp. 1–15. ISBN: 978-3-030-48258-9. DOI: 10.1007/978-3-030-48259-6_1 (cit. on p. 6).
- [20] Omar Mohamed. «Optimization of fused deposition modeling process parameters: a review of current research and future prospects». In: *Advances in Manufacturing* 3 (Feb. 2015), pp. 42–52. DOI: 10.1007/s40436-014-0097-7 (cit. on p. 6).
- [21] T. Editors of Encyclopaedia. «Polymer». In: *Encyclopedia Britannica*. Ed. by T. Editors of Encyclopaedia. Britannica, Aug. 2022. URL: <https://www.britannica.com/science/polymer> (cit. on p. 6).
- [22] Joamin Gonzalez-Gutierrez, Santiago Cano, Stephan Schuschnigg, Christian Kukla, Janak Sapkota, and Clemens Holzer. «Additive Manufacturing of Metallic and Ceramic Components by the Material Extrusion of Highly-Filled Polymers: A Review and Future Perspectives». In: *Materials* 11.5 (2018). ISSN: 1996-1944. DOI: 10.3390/ma11050840. URL: <https://www.mdpi.com/1996-1944/11/5/840> (cit. on p. 7).
- [23] Marius A. Wagner, Amir Hadian, Tutu Sebastian, Frank Clemens, Thomas Schweizer, Mikel Rodriguez-Arbaizar, Efrain Carreño-Morelli, and Ralph Spolenak. «Fused filament fabrication of stainless steel structures - from binder development to sintered properties». In: *Additive Manufacturing* 49 (2022), p. 102472. ISSN: 2214-8604. DOI: <https://doi.org/10.1016/j>

- addma.2021.102472. URL: <https://www.sciencedirect.com/science/article/pii/S2214860421006229> (cit. on p. 8).
- [24] Zhangwei Chen et al. «3D printing of ceramics: A review». In: *Journal of the European Ceramic Society* 39.4 (2019), pp. 661–687. ISSN: 0955-2219. DOI: <https://doi.org/10.1016/j.jeurceramsoc.2018.11.013>. URL: <https://www.sciencedirect.com/science/article/pii/S0955221918306782> (cit. on p. 8).
- [25] Hussien Hegab. «Design for additive manufacturing of composite materials and potential alloys: A review». In: *Manufacturing Review* 3 (Jan. 2016), p. 11. DOI: [10.1051/mfreview/2016010](https://doi.org/10.1051/mfreview/2016010) (cit. on p. 8).
- [26] Sunpreet Singh, Seeram Ramakrishna, and Roopkaran Singh. «Material issues in additive manufacturing: A review». In: *Journal of Manufacturing Processes* 25 (Jan. 2017), pp. 185–200. DOI: [10.1016/j.jmapro.2016.11.006](https://doi.org/10.1016/j.jmapro.2016.11.006) (cit. on pp. 9, 11).
- [27] Pranjal Jain and A.M. Kuthe. «Feasibility Study of Manufacturing Using Rapid Prototyping: FDM Approach». In: *Procedia Engineering* 63 (2013). The Manufacturing Engineering Society International Conference, MESIC 2013, pp. 4–11. ISSN: 1877-7058. DOI: <https://doi.org/10.1016/j.proeng.2013.08.275>. URL: <https://www.sciencedirect.com/science/article/pii/S1877705813014884> (cit. on p. 10).
- [28] Rahito Suryo Wasono, Dzuraidah Abd Wahab, and Abdul Hadi Azman. «Additive Manufacturing for Repair and Restoration in Remanufacturing: An Overview from Object Design and Systems Perspectives». In: *Processes* 7 (Nov. 2019), p. 802. DOI: [10.3390/pr7110802](https://doi.org/10.3390/pr7110802) (cit. on p. 10).
- [29] URL: https://www.stratasys.com/en/resources/resource-guides/?filter=RT_Fused_Deposition_Modeling+RR_Whitepaper+RR_Case_study+RI_Automotive (cit. on p. 10).
- [30] URL: https://www.stratasys.com/en/resources/resource-guides/?filter=RT_Fused_Deposition_Modeling+RR_Whitepaper+RR_Case_study+RI_Aerospace (cit. on p. 10).
- [31] *Roboze ULTEMTM - Scheda Tecnica (ver. 1.0)*. Roboze. 2021 (cit. on pp. 10, 17, 52).
- [32] Jingjunjiao Long, Hamideh Gholizadeh, Jun Lu, Craig Bunt, and Ali Seyfodin. «Review: Application of Fused Deposition Modelling (FDM) Method of 3D Printing in Drug Delivery». In: *Current pharmaceutical design* 22 (Oct. 2016). DOI: [10.2174/1381612822666161026162707](https://doi.org/10.2174/1381612822666161026162707) (cit. on p. 11).

- [33] Conor Whlean and Con Sheahan. «Using Additive Manufacturing to Produce Injection Moulds Suitable for Short Series Production». In: *Procedia Manufacturing* 38 (2019). 29th International Conference on Flexible Automation and Intelligent Manufacturing (FAIM 2019), June 24-28, 2019, Limerick, Ireland, Beyond Industry 4.0: Industrial Advances, Engineering Education and Intelligent Manufacturing, pp. 60–68. ISSN: 2351-9789. DOI: <https://doi.org/10.1016/j.promfg.2020.01.008>. URL: <https://www.sciencedirect.com/science/article/pii/S2351978920300081> (cit. on p. 11).
- [34] M.A. León-Cabezas, A. Martínez-García, and F.J. Varela-Gandía. «Innovative functionalized monofilaments for 3D printing using fused deposition modeling for the toy industry». In: *Procedia Manufacturing* 13 (2017). Manufacturing Engineering Society International Conference 2017, MESIC 2017, 28-30 June 2017, Vigo (Pontevedra), Spain, pp. 738–745. ISSN: 2351-9789. DOI: <https://doi.org/10.1016/j.promfg.2017.09.130>. URL: <https://www.sciencedirect.com/science/article/pii/S2351978917307655> (cit. on p. 11).
- [35] 2022. URL: <https://www.roboze.com/it/> (cit. on p. 15).
- [36] *Roboze Carbon PEEK - Scheda Tecnica (ver. 1.0)*. Roboze. 2021 (cit. on pp. 16, 50, 52).
- [37] S. O’Neill and M. Kilic. «Discontinuous Long-Fiber (DLF) Thermoplastic Composite Replacement for Complex-Shape Metallic Helicopter Fairing Rib». In: *Sampe Journal* 52 (Sept. 2016), pp. 28–35 (cit. on p. 16).
- [38] Solvay. *Carbon-Filled PEEK Grade Offering Enhanced Performance for Braking Systems*. Aug. 2021. URL: <https://www.iem.eu/article/carbon-filled-peek-grade-offering-enhanced-performance-for-braking-systems/> (cit. on p. 16).
- [39] *Explore the Possibilities with Carbon PEEK Material properties*. 2022. URL: <https://readingplastic.com/carbon-peek-material-properties/> (cit. on p. 16).
- [40] Fast Radius. *Aerospace meets additive: Everything you need to know about ULTEM™(PEI)*. Feb. 2020. URL: <https://www.fastradius.com/resources/everything-ultem/> (cit. on p. 17).
- [41] F. Gualdo. *ULTEM 9085*. July 2016. URL: <https://www.spring-italia.com/materiale-ultem-9085/> (cit. on p. 18).
- [42] CMG. *PEI Polyetherimide ULTEM™*. 2020. URL: <https://www.piedmontcmg.com/material-selection-guide/ultem-pei-polyetherimide/> (cit. on p. 18).

- [43] *ISO/ASTM 52902: Additive manufacturing - Test artifacts - Geometric capability assessment of additive manufacturing systems*. July 2019. DOI: 10.1520/52902-19 (cit. on p. 19).
- [44] Muammel Hanon, Robert Marczis, and L. Zsidai. «Influence of the 3D printing process settings on tensile strength of PLA and HT-PLA». In: *Periodica Polytechnica, Mechanical Engineering* 65 (Nov. 2020), pp. 38–46. DOI: 10.3311/PPme.13683 (cit. on p. 50).
- [45] *ASTM D638: Standard Test Method for Tensile Properties of Plastics*. Mar. 2015. DOI: 10.1520/D0638-14 (cit. on p. 52).
- [46] Albert Forés-Garriga, Marco A. Pérez, Giovanni Gómez-Gras, and Guillermo Reyes-Pozo. «Role of infill parameters on the mechanical performance and weight reduction of PEI Ultem processed by FFF». In: *Materials & Design* 193 (2020), p. 108810. ISSN: 0264-1275. DOI: <https://doi.org/10.1016/j.matdes.2020.108810>. URL: <https://www.sciencedirect.com/science/article/pii/S0264127520303440> (cit. on p. 52).
- [47] Giulia Morettini, Massimiliano Palmieri, Lorenzo Capponi, and Luca Landi. «Comprehensive characterization of mechanical and physical properties of PLA structures printed by FFF-3D-printing process in different directions». In: *Progress in Additive Manufacturing* 7 (Mar. 2022), pp. 1–12. DOI: 10.1007/s40964-022-00285-8 (cit. on p. 52).